UNIVERSITY OF CALIFORNIA SAN DIEGO

Distinct and conserved regions on the multi-domain Ulp2 regulate the substrate specificity of Ulp2 at the rDNA

A thesis submitted in partial satisfaction of the
requirements for the degree Master of Science

in

Biology

by

Wei-Tsung Yuan

Committee in charge:

Professor Huilin Zhou, Chair
Professor Eric Bennett, Co-Chair
Professor Yunde Zhao

2019

The thesis of Wei-Tsung Yuan is approved, and it is acceptable in quality and form for publication on microfilm and electronically:

_____

_____

Co-Chair

_____

Chair

University of California San Diego
2019

Table of Contents

List of Figures

Acknowledgements

I would like to acknowledge Dr. Huilin Zhou for his mentoring and support.

I would like to thank Dr. Claudio Albuquerque for the countless lessons he taught me in approaching experiments.

I would like to thank members of Zhou lab and the previous works that made this publication possible.

Section 2.2.1 describes a growth analysis a growth analysis and experiments addressing the Ulp2 protein abundance and the cell cycle profile of *ulp2* C-terminal mutants that were designed and performed by Dr. Raymond T. Suhandynata.

Section 2.2.2 describes a binding assay that was designed and performed by Dr. Claudio ponte de Albuquerque.

In Section 2.2.3, the competitive inhibition of SUMO protease activity by SIM peptide described section was designed and performed by Dr. Claudio ponte de Albuquerque.

In Section 2.2.4, the SUMO protease assay on *in vitro* generated polySUMO that was designed by Dr. Claudio ponte de Albuquerque, and the purification of endogenous sumoylated protein and the SUMO protease assay on endogenous sumoylated protein described in this section were designed and performed by Dr. Claudio ponte de Albuquerque.

Section 2.2.5 describes MS experiments designed performed and analyzed by Dr. Claudio ponte de Albuquerque and Dr. Raymond T. Suhandynata.

Dr. Huilin Zhou designed the approach to use catalytically inactive Ulp1 to purify sumoylated protein from whole cell extracts in Section 3.2.1.

Chapter 2, in part, contains material as it appears in Binding to small ubiquitin-like modifier and the nucleolar protein Csm1 regulates substrate specificity of the Ulp2 protease 2018. de Albuquerque, C. P.; Suhandynata, R. T.; Carlson, C. R.; Yuan, W. T.; Zhou, H., J Biol Chem, 2018.

Abstract of the Thesis

Distinct and conserved regions on the multi-domain Ulp2 regulate the substrate specificity of Ulp2 at the rDNA

by

Wei-Tsung Yuan

Master of Science in Biology

University of California San Diego, 2018

Professor Huilin Zhou, Chair
Professor Eric Bennett, Co-Chair

Protein post-translational modification by small ubiquitin-like modifier (SUMO) is a highly-conserved process in all eukaryotes and is regulated both by the SUMO conjugating enzymes and the desumoylating enzymes. In yeast, the two SUMO proteases—Ulp1 and Ulp2—perform the entirety of the desumoylation in the cell. Ulp1 is known to perform the majority of the desumoylation in the cell, and its catalytic domain appears to bind to SUMO directly. Ulp2 is known to suppress polysumoylated proteins in the cell and appears to target proteins at three specific regions in the cell: at the rDNA, the kinetochore and the origins of replication. The mechanism through which Ulp2 orchestrates its substrate specificity has not been well characterized, however. In the first part of this dissertation, I demonstrated that

the Ulp2 C-terminal conserved region is a SUMO interacting motif, which facilitates Ulp2 in desumoylating polysumoylated substrates. In the second part of this dissertation, I showed that the catalytically inactivated Ulp1 can be used to purify endogenous sumoylated protein from the cell.

Chapter 1:

Introduction to the SUMO pathway, the two SUMO proteases in *S. cerevisiae*

1.1 General Overview of the SUMO pathway

The Small Ubiquitin-like Modifier (SUMO), a member of the family of Ubiquitin-like proteins (UbLs), is a post-translational modification (PTM) that is essential for various cellular processes and is conserved across all eukaryotes. SUMO, like many other members of the UbLs, possesses high structural similarities to ubiquitin while only sharing minimal amino acid sequence identity (Bayer et al., 1998; Mossessova & Lima, 2000). In *S. cerevisiae*, only one SUMO protein is known to exist which is encoded by *SMT3*, while in the mammalian cells, multiple SUMO paralogs are known and are encoded by four isoforms SUMO-1, -2, -3 and -4. In both *S. cerevisiae* and mammals, SUMO is first expressed as a precursor with several additional amino acids on its C-terminal appendage, and requires SUMO processing on its C-terminal appendages to expose a di-glycine (-GG) motif for subsequent conjugation.

Like most UbL-modification enzymatic mechanisms, SUMO conjugation involves a cascade of three enzymes: an ATP dependent E1-activating enzyme, an E2-conjugating enzyme and an E3-Ligase (Figure 1.1). In the initial activation reaction, the heterodimeric SUMO E1 enzyme (Aos1/Uba2) facilitates the formation of a short lived adenylated SUMO intermediate, SUMO-GG C-terminal carboxyl-AMP. The SUMO-GG of this intermediate is quickly transferred onto a conserved cysteine residue on the E1 enzyme, forming a high-energy thioester bond (E1~SUMO) and releasing an AMP. E1 thioester SUMO can then readily transfer SUMO onto the catalytic cysteine of E2 (Ubc9), forming another thioester bond (E2~SUMO). In *S. cerevisiae* and mammals, each of the heterodimeric E1 subunits and the E2 enzyme

is encoded by one gene—Aos1/Uba2 (known as Sae1 and Sae2 in mammals) and Ubc9. In the final step of the conjugation process, substrate-selective SUMO conjugation relies on the E3-ligase. Like the Ubiquitin E3-ligases, the SUMO E3-ligase does not participate in the direct catalysis of the SUMO-conjugation process, instead acting as a platform to bring E2-SUMO and the substrate in proximity to each other. Several E3-ligases have been recognized in both *S. cerevisiae* and mammals, most of which contain an SP-RING domain. Although it has been shown that E1 and E2 alone can perform SUMO conjugation *in vitro*, SUMO E3-ligase is required for ligase activity *in vivo* (Reverter & Lima, 2005). This is due to the E3 SP-RING domain, which functions primarily in activating the E2-SUMO (Hochstrasser, 2001; Yunus & Lima, 2009). In *S. cerevisiae*, the SP-RING bearing E3-ligases consist of three mitotic E3-ligases (Siz1, Siz2 and Mms21), and a meiotic-specific E3-ligase (Zip3) (Johnson & Gupta, 2001; Takahashi, Kahyo, Toh, Yasuda, & Kikuchi, 2001; Zhao & Blobel, 2005). In mammals, the SP-RING bearing E3-ligases contain five distinctive PIAS (protein inhibitor of activated STAT) family E3-ligases and Mms21 (also known as Nse2). Moreover, it has been shown that the substrate selective E3-ligases have partial functional overlaps in both *S. cerevisiae* (Albuquerque et al., 2013; Reindle et al., 2006) and mammals (Bylebyl, Belichenko, & Johnson, 2003; Reverter & Lima, 2005).

At the end of this SUMO conjugating cascade, the C-terminal carboxyl end of the SUMO-GG is conjugated onto the ε-amine on lysine residues of the substrate through an isopeptide bond. Aside from SUMO conjugation at the lysine residues of the sumoylated substrate, SUMO conjugation can also occur with lysine residues of

another SUMO, usually already conjugated to a protein substrate. These polymeric SUMO-SUMO conjugations on sumoylated substrates are often referred to as polySUMO chains. In other instances, a sumoylated protein can have multiple SUMO conjugations at different lysine residues of the sumoylated protein.

The removal of SUMO substrates is achieved by one single group of enzymes, the SUMO proteases, in an energy-independent process known as SUMO deconjugation. Additionally, the SUMO proteases also perform the essential role of cleaving the peptide bond of the SUMO C-terminal extension on the SUMO precursor to expose the di-glycine motif, known as SUMO maturation. In *S. cerevisiae*, there are two SUMO proteases, Ulp1 and Ulp2 (Li & Hochstrasser, 1999, 2000). In mammals, there are six SUMO proteases: four Ulp1 homologs, SENP1, -2, -3 and -5, and two Ulp2 homologs, SENP6 and -7. In both *S. cerevisiae* and mammalian cells, various evidence from prior studies demonstrates that the SUMO proteases differ in their intracellular localizations and substrate preferences, suggesting that the SUMO proteases may exhibit distinct and non-overlapping functions.

Together, the SUMO conjugating enzymes and SUMO proteases constitute the SUMO system, which regulates SUMO homeostasis within the cell. The SUMO pathway involving sumoylation and desumoylation is essential in mediating many cellular processes and functions. Numerous SUMO modified proteins have been identified to date that involve various critical cellular processes in the eukaryotic cell, including transcription control, chromatin transcriptional regulation, nuclear-cytosolic transport, DNA repair and protein-protein interactions (Hardeland, Steinacher,

Jiricny, & Schar, 2002; Matunis, Coutavas, & Blobel, 1996; Nathan et al., 2006; Shiio & Eisenman, 2003; Song, Durrin, Wilkinson, Krontiris, & Chen, 2004). However, despite many recent studies that shed light on many aspects of the SUMO system, the diverse biological functions that SUMO conjugation serves have in many cases yet to be determined.

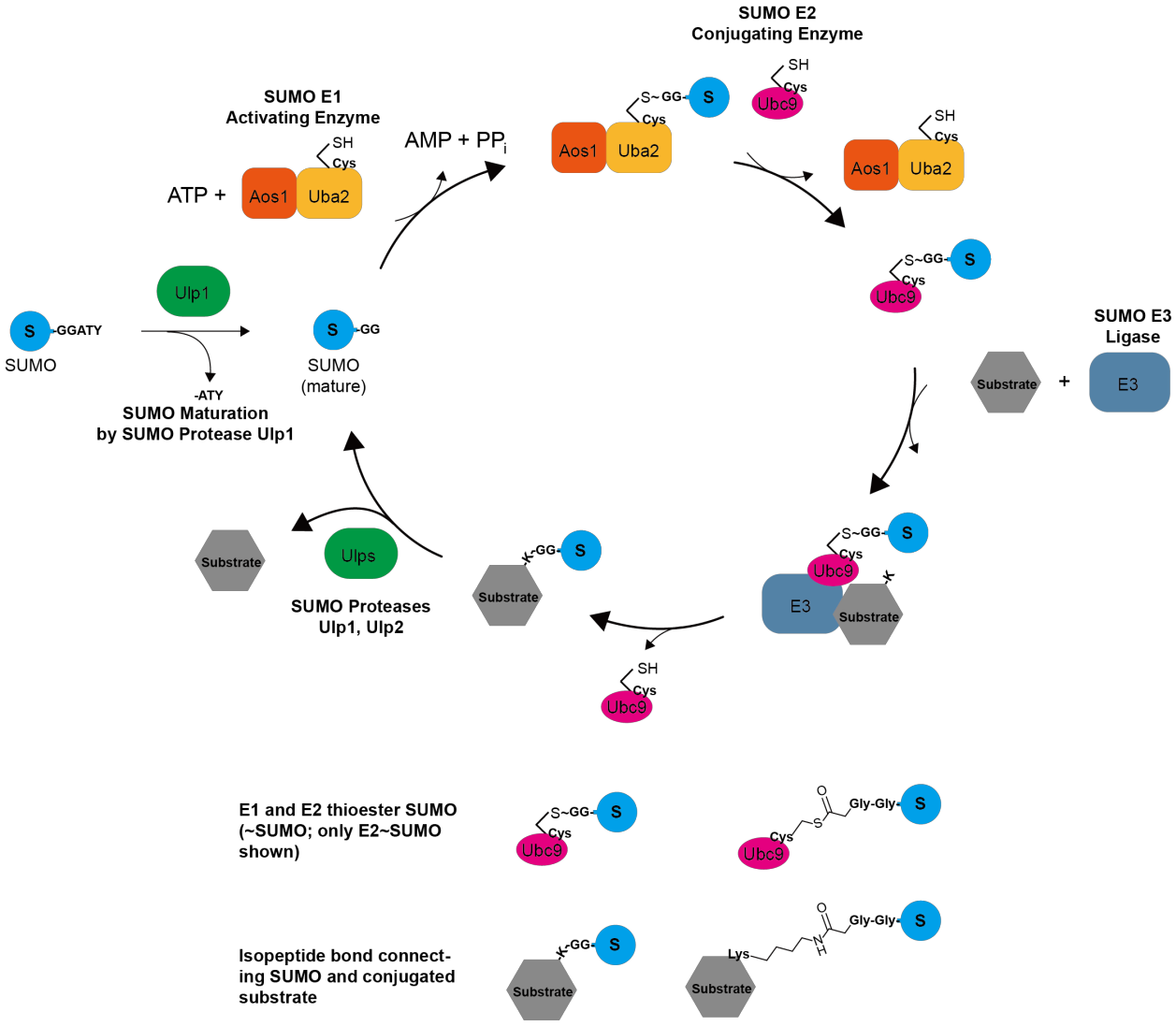

Figure 1.1: Overview of SUMO pathway. Protein post-translational modification by small ubiquitin-like modifier (SUMO) is conjugated by the three cascade of SUMO conjugating enzymes: the E1 activating enzyme (Aos1:Uba2), the E2 conjugating enzyme (Uba2), the E3 ligases; it is deconjugated by the SUMO proteases (Ulp1 and Ulp2).

1.2 The Ubiquitin-like specific proteases (Ulp1 and Ulp2) in *S. cerevisiae*

In the mammalian SUMO systems, the sheer number of SUMO proteases and isoforms of SUMO revealed that each of the SUMO proteases preferentially acts on different SUMO isoforms and towards either SUMO deconjugation or maturation activity (Hickey, Wilson, & Hochstrasser, 2012). However, the degree of complexity is reduced in *S. cerevisiae* which only expresses two SUMO proteases, Ulp1 and Ulp2, and possesses only one SUMO encoding gene *SMT3.* Since only two SUMO proteases have been identified in *S. cerevisiae*, it is believed that Ulp1 and Ulp2 perform all of the SUMO deconjugation and maturation processes within the cell. Strikingly, recent structural analyses reveal that a high degree of structural organization is retained between each of the *S. cerevisiae* SUMO proteases and their mammalian paralogs (Reverter & Lima, 2004, 2006; Shen, Dong, Liu, Naismith, & Hay, 2006). Thus, defining the mechanism by which the two *S. cerevisiae* SUMO proteases achieve their *in vivo* specificities likely can provide considerable insight into understanding the diverse biological functions of the SUMO system in both *S. cerevisiae and* mammals.

In previous genetic studies in yeast, mutations in either Ulp1 or Ulp2 revealed that the two SUMO proteases likely exhibit distinct substrate specificity and functional roles as distinct patterns of sumoylated substrates accumulate in each mutant background and each mutant exhibits unique defects (Li & Hochstrasser, 1999, 2000). Later studies concerning the localization and biochemical activity of the yeast SUMO proteases Ulp1 and Ulp2 reveal that Ulp1 is involved in SUMO

maturation and SUMO deconjugation while Ulp2 primarily cleaves the isopeptide-linked polySUMOs (Bylebyl et al., 2003; Li & Hochstrasser, 2000, 2003).

The role of Ulp1 in SUMO maturation is known to be essential for viability of the cell. Yet, in Ulp1 deletion cells, the inviability of the *ulp1Δ* phenotype cannot be rescued in a genetic background expressing mature SUMO (SUMO-GG) (Li & Hochstrasser, 1999). The inviability of the *ulp1Δ* SUMO-GG phenotype suggests thatUlp1 is essential to the cell outside of SUMO maturation. Strikingly, our lab recently demonstrated that the lethality of a *ulp1Δ* mutant can be rescued by *siz1Δsiz2Δ* double mutant in the SUMO-GG background (de Albuquerque, Liang, Gaut, & Zhou, 2016). It has been shown that Siz1 and Siz2, the two SUMO E3-ligases, are known to conjugate the majority of the sumoylated substrates in the cell (Albuquerque et al., 2013; de Albuquerque et al., 2016; Reindle et al., 2006). The viability of a *ulp1Δ* mutant in a *siz1Δsiz2Δ*SUMO-GG background indicates that the essential function of Ulp1 can also be attributed to its role in keeping intercellular sumoylation sufficiently low in addition to its role in SUMO maturation. Notably, a considerable accumulation of global sumoylation still occurred in a *ulp1Δ* mutant in the Siz1ΔSiz2Δ SUMO-GG background, comparable to that found in wildtype (WT) cells (de Albuquerque et al., 2016). This finding suggests that Ulp1 not only antagonizes the conjugation of SUMO by Siz1 and Siz2, but also performs the majority of global desumoylation. Previous studies have also demonstrated that Ulp1 exhibits highly potent activity in desumoylating purified SUMO substrates in vitro (Li & Hochstrasser, 1999, 2003), and this potent activity can be attributed to the tight binding between SUMO and Ulp1's catalytic domain which has been crystallized

(Mossessova & Lima, 2000). Strikingly, Elmore and colleagues showed that the inactive Ulp1 catalytic domain with the C580S mutation binds tightly to sumoylated proteins and can be used to purify endogenous sumoylated protein, providing a valuable tool to study protein sumoylation(Elmore et al., 2011). We modified the method used by Elmore and colleagues and showed that we could detect Mcm16 sumoylation in a one-step purification in Chapter 3. In summary, these findings provided a considerable understanding of the function of Ulp1 and established Ulp1 as playing a major role in mediating global SUMO homeostasis.

Although Ulp2 is not essential for viability, the loss of Ulp2 causes various growth defects unique to the *ulp2Δ* mutant background (Li & Hochstrasser, 2000) as well as a tendency to rapidly accumulate suppressor mutations with specific aneuploidy effects as shown by more recent analyses (Ryu, Wilson, Mehta, Hwang, & Hochstrasser, 2016). While the tendency of *ulp2Δ* mutants to accumulate suppressor mutations renders its functional analysis difficult, the growth defect in *ulp2Δ* seems to be rescued by mutations that negatively affect polySUMO chain formation (Bylebyl et al., 2003; Ryu et al., 2016). Interestingly, quantitative proteomic data shows that Ulp2 is a highly specific SUMO protease and targets specific protein complexes involved in distinct and essential cellular processes, including ribosomal DNA (rDNA) maintenance, chromosomal segregation, and DNA replication (Albuquerque et al., 2013; de Albuquerque et al., 2016). In addition, the loss of Ulp2 resulted in drastic increases of sumoylated proteins associated at these three distinct sets of Ulp2 substrates when compared to the wildtype.

Among the known substrates of Ulp2, its rDNA associated substrates have been better characterized to date. Substantial genetic and biochemical data have suggested that the rDNA-silencing networks are regulated by the SUMO pathway. In our previous study, quantitative mass spectrometry (MS) analysis revealed that Ulp2 selectively desumoylates specific rDNA-associated proteins (Tof2, Cdc14 and Net1) at the nucleolus (de Albuquerque et al., 2016). In agreement with our results, several other groups have also reported that rDNA silencing proteins are sumoylated, including several other proteins that associate to the rDNA locus, such as Fob2 and Sir2 (Albuquerque et al., 2013; Cremona et al., 2012; de Albuquerque et al., 2016; Gillies et al., 2016; Reindle et al., 2006; Srikumar, Lewicki, & Raught, 2013). Furthermore, in our recent work that sought to understand how Ulp2 demonstrates such substrate specificity, we showed that Ulp2 is directed to the rDNA regions through its Csm1 binding domain and subsequently regulates the abundance of the rDNA associated proteins together with the heterodimeric SUMO-targeted ubiquitin ligases Slx5:Slx8. In short, the abundance of sumoylated Tof2 is down-regulated by the SUMO-targeted ubiquitin ligases (STUbLs), which mediate the ubiquitin dependent degradation of sumoylated Tof2, and this process is antagonized by the isopeptidase activity of Ulp2 (Liang et al., 2017; Sriramachandran & Dohmen, 2014). This SUMO-dependent regulation of Tof2 is required for the proper maintenance of rDNA at the rDNA-silencing networks. In Ulp2 mutants that fail to bind to Csm1, sumoylated Tof2 is rapidly degraded and the cells displays an rDNA silencing defect. In addition, we observe a concurrent accumulation of sumoylated Cdc14 and Net1, suggesting that the C-terminal Csm1 binding domain contributes to Ulp2's substrate specificity for its nucleolar

substrates. However, substantially more sumoylation of nucleolar substrates was seen to accumulate in *ulp2Δ* strains (Gillies et al 2016, Albuquerque et al. 2013, de Albuquerque et al. 2016). Collectively, these observations strongly implicate SUMO as playing a significant role in regulating the maintenance of rDNA; however, the underlying mechanism by which Ulp2 is recruited to the rDNA can only be partially explained by its Csm1 binding domain.

Despite our current understanding of Ulp1 and Ulp2, the mechanism by which such specificity is orchestrated *in vivo* remains unresolved. One insight into this intricate specificity observed *in vivo* is related to the subcellular localization of these proteins. Prior studies showed that both Ulp1 and Ulp2 localize to the nucleus via N-terminal nuclear localization signals (NLS) with Ulp1 localizing to the inner surface of the nuclear pore complex (NPC) and Ulp2 localizing to the nucleoplasm (Kroetz, Su, & Hochstrasser, 2009; Li & Hochstrasser, 2003). Moreover, it has been suggested that the Ulp2 C-terminal domain (CTD) contains a SIM (SUMO interacting motif), a consensus defined by I/V-X-I/V-I/V and usually flanked on one side by a cluster of acidic residues (Hannich et al., 2005; Kroetz et al., 2009; Song et al., 2004). Although no experimental data is available, this putative SIM on Ulp2 CTD could play a role in enabling Ulp2 to specifically target polySUMO substrates (Bylebyl et al., 2003). Importantly, the role of this putative SIM on the substrate specificity of Ulp2has yet to be investigated.

Chapter 2:

Conserved regions—Ulp2 C-terminal SIM and the Csm1-binding domain—regulate Ulp2 substrate specificity toward its rDNA-associated substrates

2.1 Introduction

The Ulp2 SUMO protease contains a large and poorly conserved N-terminal region and a largely unstructured C-terminal extension on either side of its catalytic domain, while the Ulp2 Csm1-binding domain in Ulp2 C-terminal identified in our previous study contains several conserved hydrophobic residues necessary for its binding to Csm1 and contributes its recruitment to its nucleolar targets (Liang et al., 2017). Although Ulp2's Csm1-binding domain is essential for the nucleolar localization of Ulp2 and acts to antagonize Slx5:Slx8 for proper maintenance of rDNA, the Ulp2 Csm1-binding domain does not seem to account for the entirety of Ulp2's substrate selectivity toward its nucleolar substrates when the defects and sumoylation levels of Ulp2 nucleolar substrates are compared between a Csm1 binding mutant (*ulp2- Δ781*) and a *ulp2* deletion mutant (*ulp2Δ*) (Liang et al., 2017). These observations suggest that although binding to Csm1 plays a partial role in desumoylating rDNA silencing proteins, we do yet not possess a comprehensive understanding of the substrate specificity of Ulp2 and further investigation is needed. To better understand how Ulp2 orchestrates its substrate selectivity, protein sequence alignment of *S. cerevisiae* Ulp2 was performed across several fungal species (Figure 1.1B). The sequence alignment revealed two conserved regions in Ulp2's C-terminal extension— $Ulp2^{725\text{-}728}$ and $Ulp2^{931\text{-}934}$—in addition to the Csm1-binding domain. One of the two conserved regions identified, $Ulp2^{725\text{-}728}$, fits the SIM consensus reported by Song and colleagues (Song et al., 2004) and will thus will be referred to as SIM ($Ulp2^{725\text{-}728}$). The other C-terminal conserved region will be referred to as the C-terminal Conserved Region (CCR).

First, we first performed a growth analysis of yeast cells with the three Ulp2 mutants containing mutations in their C-terminal conserved regions (and in combination) to investigate their roles in the function of Ulp2. Here, we determined that the three conserved regions on the Ulp2 C-terminus contain distinct and overlapping functions based on our growth analysis. We also showed that the various mutations in Ulp2 do not impact its cellular abundance or cell cycle profile in order to confirm that the defects in our growth analysis were not due to protein instability or altered cell cycle progression. We then showed that while Ulp2's C-terminal SIM binds to SUMO *in vitro* with increasing affinity toward longer SUMO chains, its C-terminal CCR cannot. An important question emerging from this result is whether Ulp2's C-terminal SIM, which can bind to SUMO *in vitro*, contributes to to Ulp2's affinity toward polySUMO *in vivo*. To address this question, we first tested whether mutations at Ulp2's C-terminal SIM influences its SUMO protease activity *in vitro* using recombinantly purified Ulp2 on either recombinantly purified linear SUMO chains, purified endogenous sumoylated protein, and in vitro synthesized polySUMO chains. Consistently, we showed that defective Ulp2 C-terminal SIM has an effect on SUMO protease activity, particularly in processing substrates with shorter SUMO chains in all three cases. Finally, we showed that mutations in theC-terminal SIM of Ulp2 result in accumulation of its nucleolar substrates, and strikingly, when combined with the Csm1-binding mutant, the resulting accumulation of its nucleolar substrates drastically increased to a level comparable to that observed in *ulp2Δ* strains.

2.2 Results

2.2.1 The three conserved regions in the Ulp2 C-terminal Domain exhibit distinct and overlapping roles

The following section describes a growth analysis and experiments addressing the Ulp2 protein abundance and the cell cycle profile of *ulp2* C-terminal mutants that were designed and performed by Dr. Raymond T. Suhandynata.

To investigate whether any of these conserved regions of Ulp2 possess any functional roles *in vivo*, we performed a growth analysis with the previously characterized F839D mutant of the Csm1-binding domain and 3 alanine (3A) mutations replacing the bulky hydrophobic residues for CCR and SIM, CCR^{3A} and SIM^{3A} (Figure 2.1A). As previously mentioned, the *ulp2Δ* mutant exhibited serious growth defects in addition to readily accumulating survivor mutants (Li & Hochstrasser, 2000; Ryu et al., 2016), suggesting that any Ulp2 mutations that impair Ulp2's functions *in vivo* can also lead to accumulation of faster growing survivors that can mask the effects of such a mutant.

In order to avoid the formation of suppressor mutations, the strain we used for growth analysis contained a complementary wildtype *ULP2* under its native promotor on a centromeric plasmid with a *URA3* maker with a *ulp2Δ* deletion at its chromosomal locus, referred to as the "shuffle" strain. Each of the Ulp2 mutations analyzed was introduced to the shuffle strain on another centromeric plasmid under its native promotor without the *URA3* marker. Treatment with 5-fluorooratic acid (5'-FOA) rapidly selects against the shuffle strain plasmid containing a wildtype copy Ulp2 (and the *URA3* marker), leaving behind only the *ulp2Δ* strain with the other centromeric plasmid-carried copies of Ulp2, which possess either *ulp2* with

mutations in the three conserved regions or the *WT ULP2*. This plasmid shuffling technique allows for the analysis of the acute effects of the mutations within 20-25 generations through the rapid removal of complementing *WT ULP2* via selection on 5'-FOA-containing media. Additionally, the Ulp2 mutant proteins and the wildtype control strain analyzed in the growth analysis contained a tandem affinity purification tag (TAP-tag), allowing subsequent analysis of the abundance of Ulp2.

Growth analysis revealed that the Ulp2 F839D mutation does impact cell growth, while both the SIM^{3A} and CCR^{3A} single mutations appear to have little to no noticeable impact on cell growth (Figure 2.1C). Strikingly, the significant cell growth defect is observed in the *ulp2* double mutants with SIM^{3A} in combination with either F839D or CCR^{3A}, while the double mutant combining F839D and CCR^{3A} does not exhibit such additive growth defect and closely resembles the minimal growth defect of the CCR^{3A} single mutant (Figure 2.1C). When all three conserved regions of Ulp2 are mutated in the triple mutant, the observed growth defect is substantial, with little to no growth on 5'-FOA media (Figure 2.1C). None of the *ulp2* mutants resulted in a reduction in the abudance of Ulp2 protein levels (Figure 2.1D). In contrast, the Ulp2 abundance in a *ulp2*-SIM^{3A}CCR^{3A} double mutant or a *ulp2* triple mutant appeared to be higher than that of the Ulp2 wildtype (Figure 2.1D). This could be due to unknown compensatory effects. Nonetheless, the growth defects observed in these Ulp2 mutants are unlikely to be attributed to their effects on the overall integrity of Ulp2 protein. In addition, we performed flow cytometry on all the *ulp2* C-terminal mutants immediately removed from 5-FOA plates (Figure 2.1C) to assay for any specific cell cycle arrest defects indicative of aberrant cell cycle progression. This was necessary

to rule out that the observed growth defects in *ulp2* C-terminal mutants could be due to cell cycle arrest. As shown in Figure 2.1E, no noticeable cell cycle arrest was observed.

Collectively, these results suggest that the three C-terminal conserved regions have specific and overlapping roles in maintaining cell growth. In particular, the C-terminal SIM likely shares a partially redundant role with either the Csm1 binding domain or the CCR in Ulp2.

Figure 2.1: The three conserved regions in the Ulp2 C-terminal Domain exhibit distinct and overlapping roles (A) Schematics of C-terminal conserved regions on the Ulp2 protease. (B) Sequence alignments of the three C-terminal conserved regions Ulp2 with its orthologs. (C) Growth defects of *ulp2* mutations compared to *WT*. Effects of mutations in Ulp2 at its three C-terminal conserved regions on cell growth are shown on a 5-FOA plate (with rapid selection against the complementing *WT ULP2* plasmid) after 3- and 5-days incubation at 30°C. Equivalent amounts of cells were also plated on YPD as a loading control after 3-days incubation at 30°C. (D) Protein abundances of mutant *ulp2* compared to *WT* post 5-FOA incubation, shown by immunoblotting for Ulp2. Loading controls are shown via Coomassie staining. (E) Cell cycle profile of each *ulp2* mutants compared to *WT* post 5-FOA incubation.

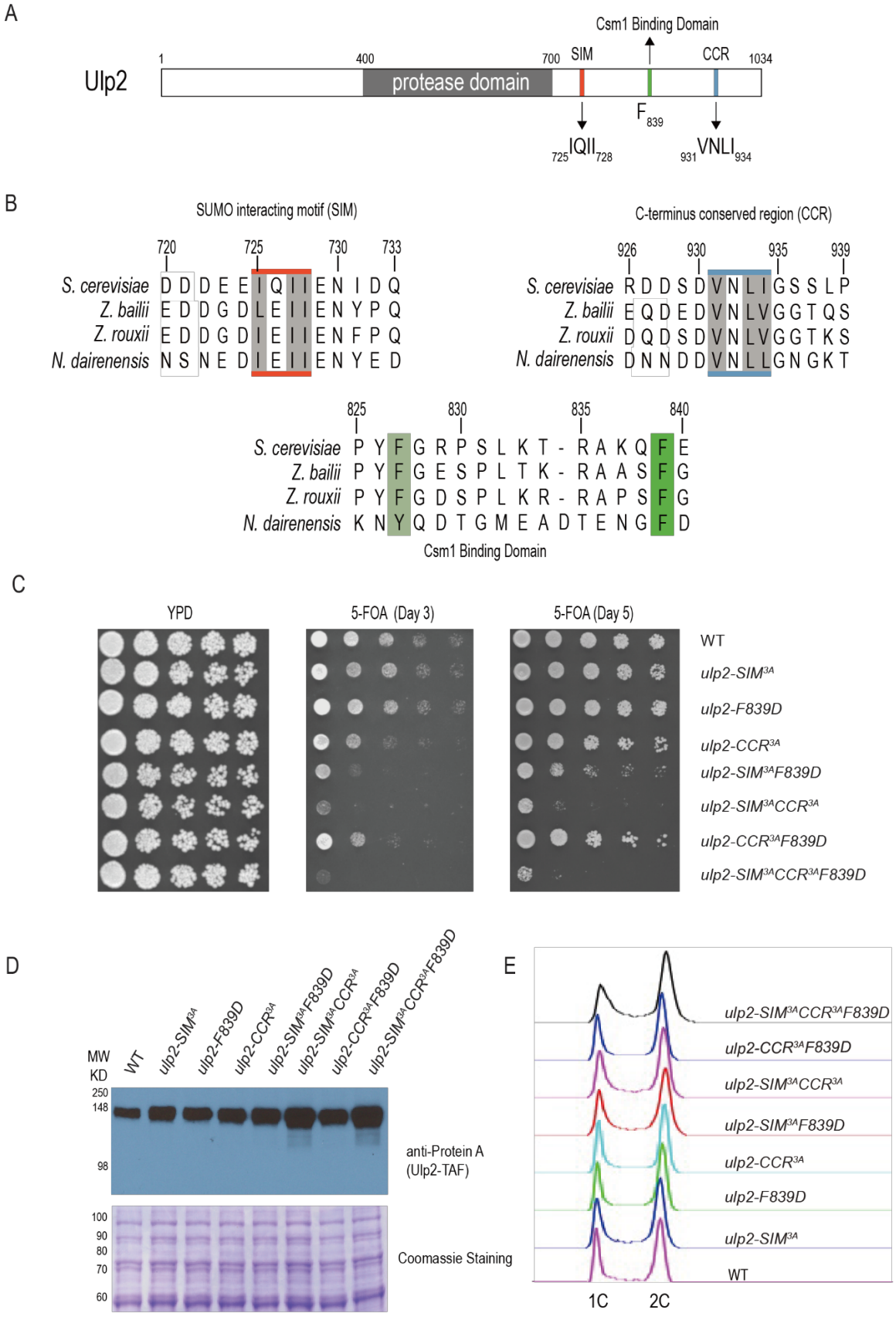
A
Csm1 Binding Domain
Ulp2
1
400
700
SIM
CCR
1034
protease domain
F 839
725 IQII 728
931 VNLI 934
B
SUMO interacting motif (SIM)
720
725
730
733
S. cerevisiae D D D E E I Q I I E N I D Q
Z. bailii E D D G D L E I I E N Y P Q
Z. rouxii E D D G D I E I I E N F P Q
N. dairenensis N S N E D I E I I E N Y E D
C-terminus conserved region (CCR)
926
930
935
939
S. cerevisiae R D D S D V N L I G S S L P
Z. bailii E Q D E D V N L V G G T Q S
Z. rouxii D Q D S D V N L V G G T K S
N. dairenensis D N N D D V N L L G N G K T
825
830
835
840
S. cerevisiae P Y F G R P S L K T - R A K Q F E
Z. bailii P Y F G E S P L T K - R A A S F G
Z. rouxii P Y F G D S P L K R - R A P S F G
N. dairenensis K N Y Q D T G M E A D T E N G F D
Csm1 Binding Domain
C
YPD
5-FOA (Day 3)
5-FOA (Day 5)
WT
ulp2-SIM3A
ulp2-F839D
ulp2-CCR3A
ulp2-SIM3AF839D
ulp2-SIM3ACCR3A
ulp2-CCR3AF839D
ulp2-SIM3ACCR3AF839D
D
MW KD
WT
ulp2-SIM3A
ulp2-F839D
ulp2-CCR3A
ulp2-SIM3AF839D
ulp2-SIM3ACCR3A
ulp2-CCR3AF839D
ulp2-SIM3ACCR3AF839D
250
148
98
anti-Protein A (Ulp2-TAF)
100
90
80
70
60
Coomassie Staining
E
ulp2-SIM3ACCR3AF839D
ulp2-CCR3AF839D
ulp2-SIM3ACCR3A
ulp2-SIM3AF839D
ulp2-CCR3A
ulp2-F839D
ulp2-SIM3A
WT
1C
2C

2.2.2 The Ulp2 C-terminal SIM functions as a SUMO interacting motif and facilitates Ulp2's binding to SUMO *in vitro*

The following section describes a binding assay that was designed and performed by Dr. Claudio ponte de Albuquerque. I helped generate the purified linear SUMO proteins that were used as substrates in the binding assay.

Although the Ulp2 C-terminal SIM had been previously suggested to function as a SUMO interacting motif based on the consensus sequence reported by Song and colleagues (Kroetz et al., 2009; Song et al., 2004), no data has indicated that Ulp2 SIM functions in SUMO binding. To determine whether Ulp2's C-terminal conserved regions—SIM and CCR—had the ability bind to SUMO, an *in vitro* binding assay was developed to probe the interaction between synthetic peptide of each of the two conserved regions and recombinantly expressed and purified linear polySUMO chains of varying length. Each of the Ulp2 C-terminal SIM and CCR biotinylated synthetic peptides for both the wildtype and the 3A mutation variants (Ulp2-SIM, -SIM^{3A}, -CCR and CCR^{3A}) were bound to NeutrAvidin resin and incubated with a mixture of linear polySUMO chains containing SUMO, 2X-SUMO, 4X-SUMO and 6X-SUMO (Figure 2.2A). As shown in Figure 2.2A, the wildtype SIM peptide binds to 4X-SUMO and 6X-SUMO, while binding is absent in the SIM^{3A} variant. Notably, the linear SUMO chains that predominantly bound to the wildtype SIM peptide was the 6x-SUMO, suggesting that there is an increase in affinity for longer linear SUMO chains. On the other hand, neither the CCR peptide or its three-alanine variant CCR^{3A} bound to any length of linear polySUMO chains (Figure 2.2B), suggesting that the Ulp2 C-terminal CCR does not play a role in the direct binding to SUMO.

The apparent increasing affinity of the C-terminal SIM of Ulp2 for longer SUMO chains prompted us to quantitatively measure the affinity between the Ulp2 SIM peptide and linear polySUMO chains of varying length. Isothermal calorimetry (ITC) was performed by injecting the Ulp2 SIM peptide into ITC cells containing SUMO, 4X-SUMO and 6X-SUMO. The resulting thermodynamic parameters were shown in Figure 2.2C-E. In the case where a single SUMO molecule was studied, the SIM peptide exhibited only a weak affinity with a K_d of 99 μM (Figure 2.2C). However, when linear polySUMO chains were used, the affinity of the Ulp2 SIM for SUMO increased dramatically; Ulp2 SIM peptide's affinity to 4X-SUMO was 2-fold greater than SUMO (K_d 52μM) and tenfold greater for 6X-SUMO than 4X-SUMO (K_d 6.5 μM) (Figure 2.2D-E). These results show that the observation that Ulp2's C-terminal SIM binds to longer linear SUMO chains (Figure 2.2A) is likely due to the increasing affinity of Ulp2's C-terminal SIM toward longer linear SUMO chains.

Furthermore, this increasing affinity for longer SUMO chains aligns with the hypothesis that Ulp2's C-terminal SIM acts as a bona fide SUMO interacting motif for Ulp2, which has been known to target polySUMO conjugates, and thus we choose to focus on the characterization of the Ulp2 C-terminal SIM in this study.

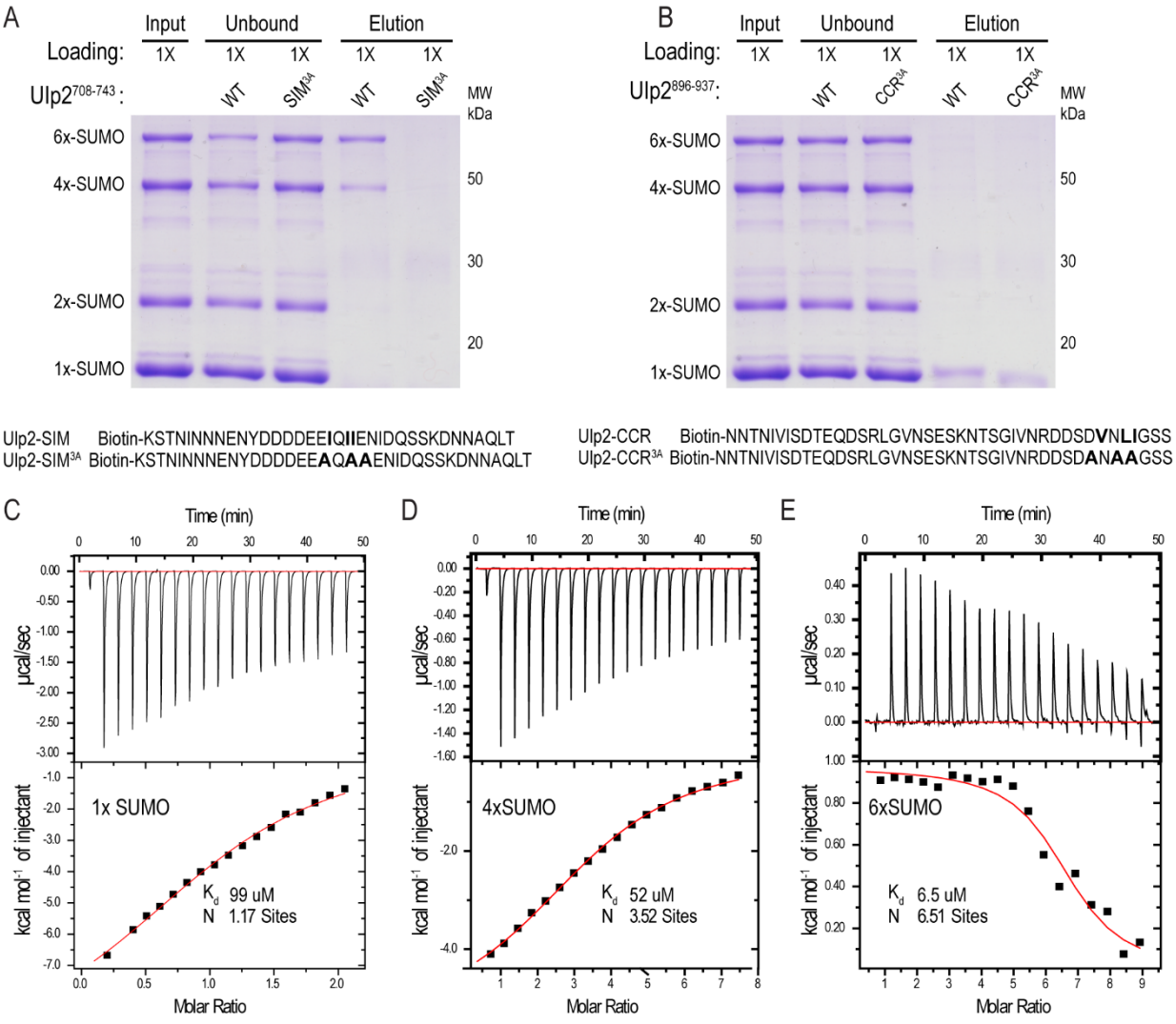

F

Average of at least two independent ITC measurements

	K_d (µM)	N	ΔH (kcal/mol)	-TΔS (kcal/mol)
1xSUMO	70 ± 30	1.13 ± 0.04	-9 ± 1	3 ± 1
4xSUMO	54 ± 2	3.3 ± 0.2	-5.5 ± 0.1	-0.29 ± 0.03
6xSUMO	4 ± 2	6.5 ± 0.1	1.3 ± 0.3	-8.8 ± 0.7

Figure 2.2: The Ulp2 C-terminal SIM peptide binds to linear SUMO chains with increasing affinity toward longer SUMO chains (A, B) Pulldown assays using Ulp2 C-terminal conserved regions and their 3A variant—SIM, SIM^{3A}, CCR and CCR^{3A} peptide—to detect binding with linear SUMO chains and effects of the 3A change to SUMO chain binding. (C-E) Isothermal titration calorimetry (ITC) showing binding between Ulp2-SIM peptide (DDDDEEIQIIENIDQSSKD) and various lengths of linear SUMO chain (1x-, 4x- and 6x-SUMO). (F) ITC summary of average fit values from at least two independent measurements.

2.2.3 The Ulp2 C-terminal SIM facilitates Ulp2 SUMO processing activity *in vitro*

The competitive inhibition of SUMO protease activity by SIM peptide described in the following section was designed and performed by Dr. Claudio ponte de Albuquerque.

The apparent increasing affinity toward longer SUMO chains for the SIM peptide observed in the binding assay and ITC measurements suggested that Ulp2's C-terminal SIM likely plays a role in Ulp2's enzymatic function, which has been known to target polySUMO or highly sumoylated conjugates *in vivo* (Bylebyl et al., 2003; Kroetz et al., 2009; Ryu et al., 2016). Since the binding assay and ITC measurements were restricted to synthetic peptides of Ulp2's C-terminal SIM, we set out to determine whether Ulp2's C-terminal SIM has a role in Ulp2's *in vitro* SUMO protease activity using recombinant Ulp2 enzymes. Attempts to purify full length Ulp2 were unsuccessful; however, a truncation of Ulp2 (residues 400-767) could be purified from bacteria that contains the catalytic domain and the C-terminal SIM, allowing us to determine whether Ulp2's C-terminal SIM plays a role in its *in vitro* SUMO protease activity.

The enzyme $Ulp2^{400\text{-}767}$ and its SIM^{3A} variant, $Ulp2^{400\text{-}767}SIM^{3A}$, are normalized together with the linear SUMO chain substrates—2x-SUMO, 4x-SUMO or 6x-SUMO—and are shown in Figure 2.3A. Although the $Ulp2^{400\text{-}767}SIM^{3A}$ contains a minor degradation product, the in vitro SUMO protease assay was normalized using the un-degraded form of the $Ulp2^{400\text{-}767}SIM^{3A}$. The *in vitro* SUMO protease assay of $Ulp2^{400\text{-}767}$ and $Ulp2^{400\text{-}767}SIM^{3A}$ were performed by incubating the mutant proteins with varying lengths of SUMO chains and quenching a portion of each reaction in

LDS-buffer at various time points (15 min, 30 min and 60 min). The *in vitro* SUMO protease activities were assessed by Coomassie staining of the quenched reaction samples after separation via SDS-PAGE. A total of 3 replicates of *in vitro* SUMO protease assay for both the Ulp2$^{400\text{-}767}$ and Ulp2$^{400\text{-}767}$SIM^{3A} mutants on each linear SUMO chain substrates were performed, and a representative set of experiments are shown in Figure 2.3E (left panels). The densitometric averages of the unprocessed SUMO chains for all 3 replicates are shown in Figure 2.3B-E (right panels).

In the case of all three linear polySUMO substrates, the SIM^{3A} mutation significantly reduced Ulp2 *in vitro* protease activity (Figure 2.3B-D). However, its effects appeared to increase as its linear SUMO substrates increased in chain length. At the final time point, wildtype Ulp2 cleaved approximately 40% more 6X-SUMO compared to Ulp2 SIM^{3A} (Figure 2.3B), but only cleaved ~30% more 4X-SUMO and ~15% more 2X-SUMO compared to Ulp2 SIM^{3A} (Figure 2.3C-3D). When comparing wildtype Ulp2's protease activity across the different linear SUMO substrates used, Ulp2 was shown to cleave longer SUMO chains more efficiently. The amount of 6X-SUMO remaining at the final time point was ~5%, while about ~55% 4X-SUMO and 75% 2X-SUMO remained (Figure 2.3C-D). Together, these observations reveal that Ulp2's C-terminal SIM enables Ulp2 to preferentially process longer SUMO chains most likely due to its increasing binding affinity for those chains.

To confirm that Ulp2's C-terminal SIM facilitates its protease activity through binding directly to SUMO, we performed a competition assay adapted from the

SUMO protease assay using various concentrations of free SIM peptide to compete with Ulp2$^{400-767}$ for binding to 6x-SUMO. If the increasing affinity of the SIM peptide for longer SUMO chains as indicated by the binding assay and ITC measurements (Figure 2.3A and 2.3C-F) enables Ulp2 to bind to substrates with longer SUMO chains, an excess of free synthetic SIM peptides should competitively bind to SUMO, and thereby inhibit the SUMO protease activity in a concentration-dependent manner. In Figure 2.4A, we show that the addition of free SIM peptide inhibited the Ulp2 SUMO protease activity on 6x-SUMO in a concentration-dependent manner. Moreover, we observed that the addition of free SIM peptide impacted the efficiency of Ulp2 SUMO protease activity significantly at each time point (Figure 2.4B and 2.4C), suggesting that the Ulp2 C-terminal SIM plays a role in recruiting SUMO chains with an increasing affinity for length and facilitates their cleavage by Ulp2's catalytic domain.

Figure 2.3: The Ulp2 C-terminal SIM facilitates Ulp2's SUMO protease activity toward linear SUMO chains (A) Coomassie staining showing linear SUMO chains and purified Ulp2$^{400-767}$ wildtype and SIM^{3A} enzymes normalized to a BSA standard. (B-D) SUMO protease assay showing the effects of the 3A-mutation on Ulp2$^{400-767}$ SIM^{3A} enzyme compared with the wildtype Ulp2$^{400-767}$ for various lengths of SUMO chains—2x-, 4x- and 6x-SUMO (D). The remaining unprocessed SUMO chains at each time point are quantified by densitometric averages of 3 independent replicates for each reaction, and are shown on the right for the corresponding reactions.

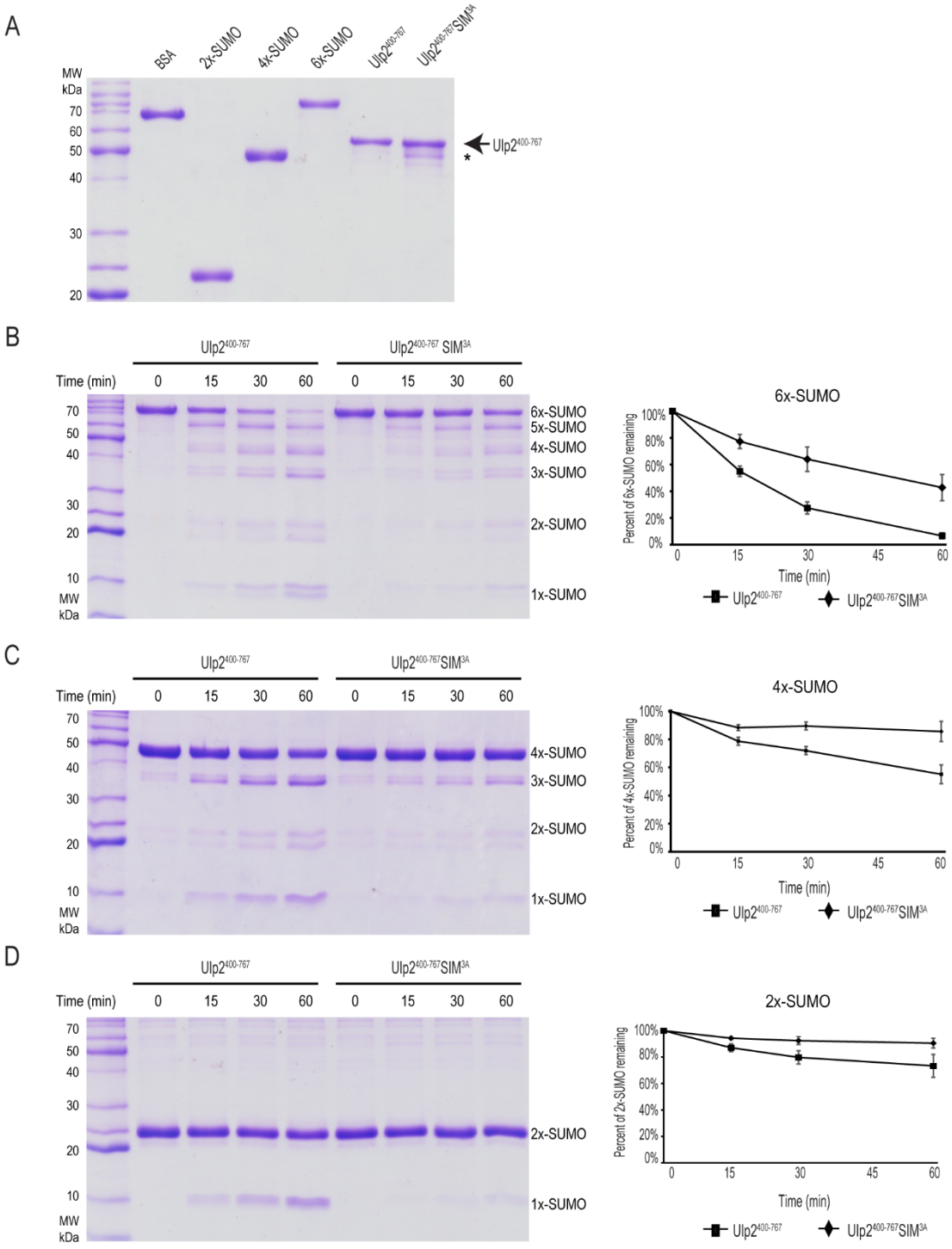
A
BSA
2x-SUMO
4x-SUMO
6x-SUMO
Ulp2400-767
Ulp2400-767SIM3A
MW kDa
70
60
50
40
30
20
Ulp2400-767
*
B
Ulp2400-767
Ulp2400-767 SIM3A
Time (min)
0
15
30
60
0
15
30
60
70
50
40
30
20
10
MW kDa
6x-SUMO
5x-SUMO
4x-SUMO
3x-SUMO
2x-SUMO
1x-SUMO
6x-SUMO
Percent of 6x-SUMO remaining
100%
80%
60%
40%
20%
0%
0
15
30
45
60
Time (min)
Ulp2400-767
Ulp2400-767SIM3A
C
Ulp2400-767
Ulp2400-767SIM3A
Time (min)
0
15
30
60
0
15
30
60
70
50
40
30
20
10
MW kDa
4x-SUMO
3x-SUMO
2x-SUMO
1x-SUMO
4x-SUMO
Percent of 4x-SUMO remaining
100%
80%
60%
40%
20%
0%
0
15
30
45
60
Time (min)
Ulp2400-767
Ulp2400-767SIM3A
D
Ulp2400-767
Ulp2400-767SIM3A
Time (min)
0
15
30
60
0
15
30
60
70
50
40
30
20
10
MW kDa
2x-SUMO
1x-SUMO
2x-SUMO
Percent of 2x-SUMO remaining
100%
80%
60%
40%
20%
0%
0
15
30
45
60
Time (min)
Ulp2400-767
Ulp2400-767SIM3A

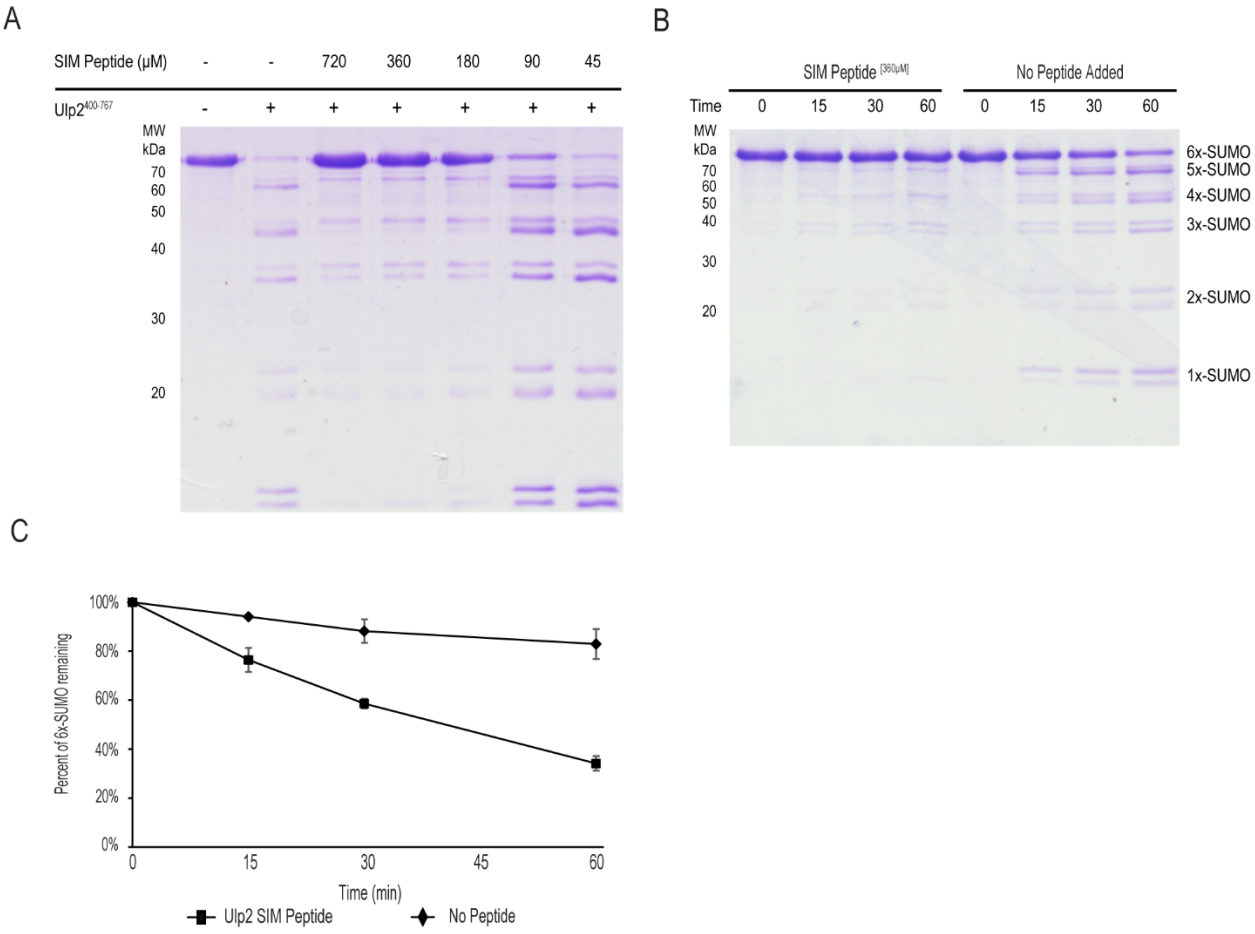

Figure 2.4: The SIM-facilitated SUMO protease activity can be inhibited by presence of Ulp2 SIM peptides (A) Effects of SIM peptide on Ulp2$^{400-767}$ SUMO protease activity shown by the SUMO protease assay with wildtype Ulp2$^{400-767}$ on 6xSUMO (as shown in Figure 2.3B) at various concentrations of SIM peptide at 60 min. post-incubation. (B) Effects of SIM peptide on Ulp2$^{400-767}$ SUMO protease activity shown by the SUMO protease assay with wildtype Ulp2$^{400-767}$ on 6xSUMO (as shown in 2.3B) at 360uM SIM peptide versus no peptide added. (C) The remaining unprocessed SUMO chains at each time point in (B) are quantified similarly (as performed in Figure 2.3B-D right panel).

2.2.4 The Ulp2 C-terminal SIM promotes desumoylation of branched polymeric SUMO chains and purified endogenous sumoylated proteins *in vitro*

The following section describes the SUMO protease assay on *in vitro* generated polySUMO that was designed by Dr. Claudio ponte de Albuquerque. The purification of endogenous sumoylated protein and the SUMO protease assay on endogenous sumoylated protein described in this section were designed and performed by Dr. Claudio ponte de Albuquerque.

Although using recombinantly expressed and purified linear SUMO chains as substrates allows easy quantification in assessing Ulp2's protease activity, almost all polySUMO chains are known to be branched through SUMO-SUMO lysine-linkages in yeast cells (Bylebyl et al., 2003) and human cells for SUMO-2 and SUMO-3 (Aillet et al., 2012; Mukhopadhyay et al., 2006). To examine this, we sought to evaluate Ulp2's protease activity toward branched polySUMO substrates. First, we synthesized polySUMO chains through an *in vitro* sumoylation reaction (Figure 2.5A), which had been shown to form branched polymeric SUMO-SUMO chains through lysine-linkages *in vitro* (Bylebyl et al., 2003). The synthesized polySUMO chains were used as substrates to evaluate the SUMO protease activity of recombinantly expressed Ulp2$^{400\text{-}767}$ and its SIM^{3A} variant. Like the SUMO protease activity shown in Figure 2.3B-D, at set time points, fractions of the reactions were isolated and quenched in LDS-buffer and subsequently analyzed by SDS-page while immunoblotting for SUMO was used to visualize the SUMO protease activity.

While wildtype Ulp2$^{400\text{-}767}$ could process all the *in vitro* synthesized branched polySUMO chains, the Ulp2$^{400\text{-}767}$ SIM^{3A} variant could not process the *in vitro* synthesized branched polySUMO chains efficiently, and resulted in an accumulation

of shorter SUMO chain byproducts in all three time points evaluated (Figure 2.5B), suggesting the Ulp2 SIM^{3A} mutation significantly reduced the ability of Ulp2 to process particularly shorter SUMO chains. Collectively, these results demonstrate the importance of Ulp2's C-terminal SIM in facilitating Ulp'2 efficient SUMO protease activity for both polySUMO linkages by peptide-bonds (Figure 2.3 and 2.4) or isopeptide-bonds (Figure 2.5B), which are particularly important for the efficient processing of shorter polySUMO chains.

Although using both linear SUMO chains or branched polySUMO chains provided us with a relatively simple method to evaluate the role of the Ulp2 SIM in its protease activity, these substrates are restricted to recombinant expression and *in vitro* synthesis, and thus may not be an ideal representation of sumoylated or polysumoylated substrates *in vivo*. To address this, we determined that there was a need to characterize the Ulp2 C-terminal SIM's role in its SUMO protease activity with endogenous substrates. Total sumoylated proteins were purified by anti-FLAG affinity resins from an *ulp2Δ* mutant with a 6xHIS-3xFLAG(HF)-SUMO background (HF-tag integrated at the 5'-end of the endogenous *SMT3* at the chromosomal locus) as shown in Figure 2.5C (Albuquerque et al., 2013). Notably, it was difficult to determine the relative amount of polysumoylated versus mono-sumoylated proteins in a purified sample that consisting of hundreds of sumoylated proteins, several of which are known to be polysumoylated Ulp2 targets (de Albuquerque et al., 2016). It has also has been shown that multiple subunits of the same protein complexes are often sumoylated together and multiple lysine residues on each of these sumoylated protein could be modified by SUMO (Johnson & Blobel, 1999), contributing to the

difficulty of determining the relative amount of each type of sumoylated species in purified sumoylated proteins. Despite these complications, the purified total sumoylated proteins were used to evaluate the SUMO protease activity of Ulp2$^{400\text{-}767}$ wildtype and its SIM^{3A} variant. As in Figure 2.5B, fractions of the reactions were isolated at distinct time points and analyzed by immunoblotting for SUMO. While the Ulp2$^{400\text{-}767}$SIM^{3A} hardly processed any endogenous sumoylated proteins, the wildtype Ulp2$^{400\text{-}767}$ processed the bulk of endogenous sumoylated proteins (Figure 2.5D). Notably, when we examined the protease activity of Ulp2$^{400\text{-}767}$ wildtype and its SIM^{3A} on endogenous sumoylated proteins, we did not observe the accumulation of shorter SUMO-chain by products such as the ones observed when the experiment was performed using *in vitro* synthesized polySUMO chains (Figure 2.5B), indicating that the amount of polysumoylated protein *in vivo* was likely too minimal to be detected. Almost all of the endogenous sumoylated protein detected by immunoblotting for SUMO likely consists of proteins that are mono-sumoylated or proteins with shorter SUMO chains. This observation indicates that these mono-sumoylated or proteins with shorter SUMO chains can be efficiently processed by Ulp2$^{400\text{-}767}$ with its wildtype SIM, while processing by Ulp2$^{400\text{-}767}$SIM^{3A} is distinctly hindered. Consistent with our results showing the protease activity of synthesized polySUMO chains, these results *indirectly* support that the Ulp2 C-terminal SIM is needed to process proteins with mono- or shorter sumoylated moieties.

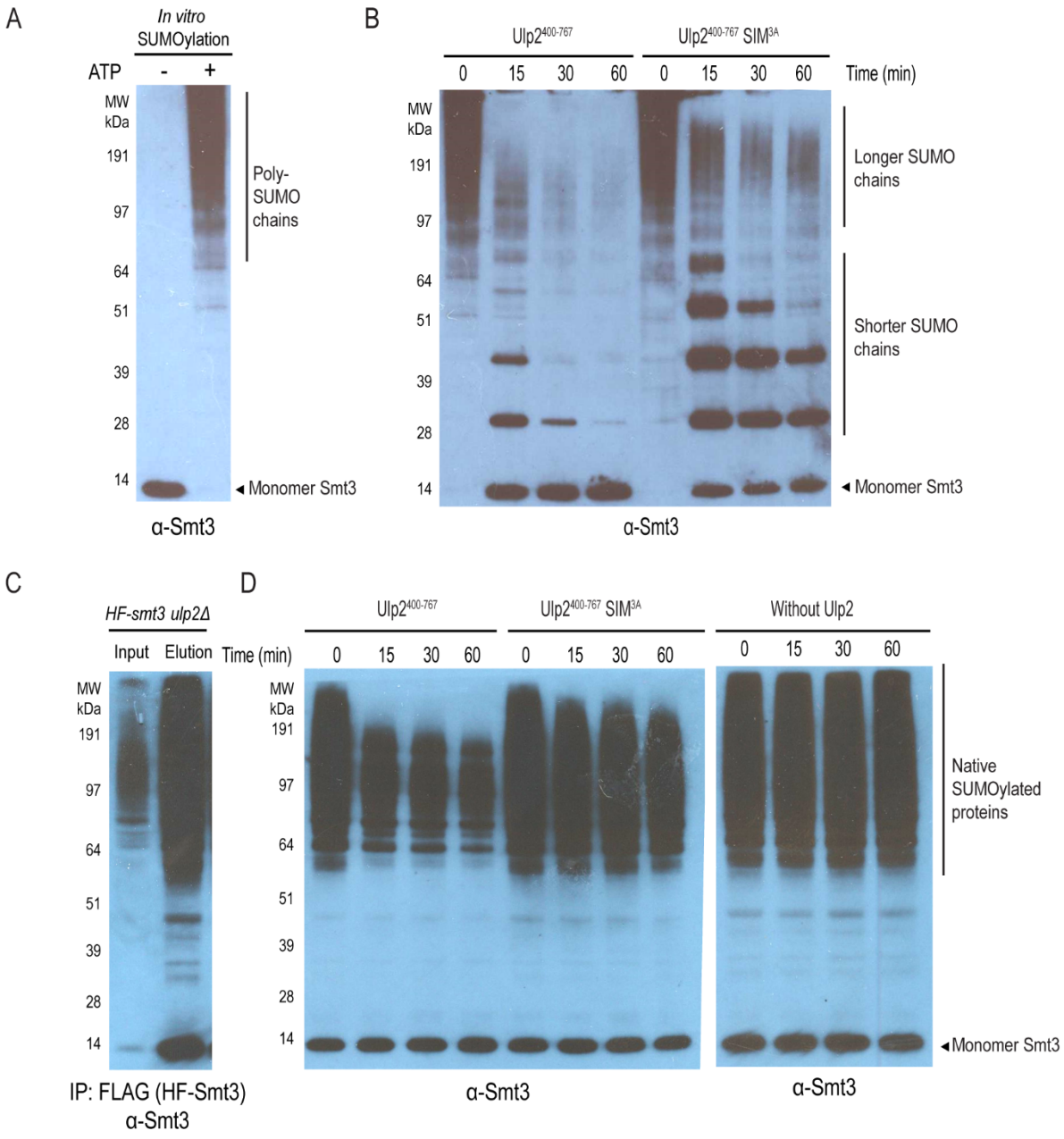

Figure 2.5: The Ulp2 C-terminal SIM facilitates its SUMO protease activity on both in vitro synthesized polySUMO chains and purified endogenous sumoylated proteins (A) PolySUMO chains generated by an *in vitro* sumoylation reaction. (B) Kinetic differences in processing *in vitro* synthesized PolySUMO chains between the wildtype SIM and 3A-SIM mutation on Ulp2$^{400-767}$ enzyme. (C) Purified endogenous sumoylated proteins from a *ulp2Δ* mutant by anti-flag affinity resin (D) Kinetic differences in processing purified endogenous sumoylated proteins between the wildtype SIM and 3A-SIM mutation on the Ulp2$^{400-767}$ enzyme.

2.2.5 Both the Ulp2 C-terminal SIM and Csm1 binding domain are required for Ulp2 to desumoylate its known nucleolar substrate *in vivo*

The following section describes MS experiments designed performed and analyzed by Dr. Claudio ponte de Albuquerque and Dr. Raymond T. Suhandynata. I did not actually perform any of the following experiments or data analysis described in the following section (2.2.5).

To evaluate the effects of the Ulp2 C-terminal SIM in processing its substrates *in vivo*, we performed a quantitative proteomic assay to determine the relative abundance of Ulp2's known sumoylated rDNA silencing proteins—Net1, Cdc14 and Tof2—in a *ulp2-SIM^{3A}* mutant. Since we had observed that the Ulp2 C-terminal SIM and the Csm1-binding domain may have specific and overlapping functions, we also determined the relative abundance of these substrates in a *ulp2-F839D* mutant and *ulp2-SIM^{3A}F839D* double mutant in addition to the *ulp2-SIM^{3A}* mutant. In our quantitative SUMO MS analysis, the *ulp2* mutant strains—*SIM^{3A}*, *F839D*, and *SIM^{3A}F839D*—were compared to *WT ULP2* strains. All strains were created in a HF-SUMO, lysine auxotrophic and arginine auxotrophic background, as described in our prior work (de Albuquerque et al., 2016; Liang et al., 2017). Using Stable Isotope Labeling via the Amino acid in Cell culture (SILAC) method, the *ulp2* mutants were grown in $^{15}N/^{13}C$-incorporated (heavy) lysine and heavy arginine while the wildtype strain was grown in $^{14}N/^{12}C$-incorporated (light) lysine and light arginine. Equal amounts of mutant and wildtype cells were mixed prior to harvesting. The clarified whole cell extracts of the mixed cells for combinations of each mutant with the wildtype were then subjected to Ni-Flag tandem affinity purification in order to purify all sumoylated protein, followed by sample preparations for liquid chromatography

(LC)-MS analysis. In principle, the relative abundance of sumoylation of any given protein in the mutant can then be determined by the abundance ratios of each of its heavy to light peptides.

Using this method, we determined the relative abundance of sumoylated Cdc14, Net1 and Tof2 (Figure 2.6B). In the *ulp2-F839D* mutant, there were no apparent changes in the abundance of sumoylated Tof2 (Figure 2.6B), and this is believed to be due to the decreased total abundance of Tof2 by STUbL Slx5:Slx8. Meanwhile, the *ulp2-F839D* mutation led to moderate increases of sumoylated Cdc14 (10 fold) and Net1 (5-fold), consistent with our prior observations (Liang et al., 2017). Moreover, we showed that the *ulp2-SIM^{3A}* mutation resulted in significant 5- to 18-fold accumulations in sumoylation across all three of the known Ulp2 nucleolar substrates (Cdc14, Net1 and Tof2) examined (Figure 2.6B). This observation suggests that the Ulp2 C-terminal SIM plays a more influential role in Ulp2's substrate specificity *in vivo* than its Csm1-binding domain. Strikingly, the double mutant, *ulp2-SIM^{3A}F839D*, resulted in a drastic increase—over 20-fold—in the abundance of sumoylated Cdc14 and Net1, which is on par with the effects of *ulp2Δ* on these proteins (de Albuquerque et al., 2016). Collectively, these observations suggest that both the Ulp2 C-terminal SIM and Csm1 binding domains are both necessary and sufficient for Ulp2 to desumoylate these known Ulp2 nucleolar substrates.

Finally, to confirm that mutations in Ulp2's C-terminal SIM and Csm1 binding domain cause a defect in processing known polysumoylated nucleolar substrates *in vivo*, we purified total sumoylated proteins from wildtype and *ulp2* mutants (*SIM^{3A}*,

F839D, and *SIM^{3A}F839D*) in the HF-SUMO Net1-3xHA background, and immunoblotted for Net1 (Figure 2.6C). In accordance with our results from the quantitative MS analysis (Figure 2.6B), *ulp2-SIM^{3A}* resulted in drastic accumulation of polysumoylated Net1 which was increased in a *ulp2-SIM^{3A}F839D* mutant, while *ulp2-F839D* showed only a slight increase in polysumoylated Net1 (Figure 2.6C). This result further validated our finding that the Ulp2 C-terminal SIM has a more important influence in desumoylation of its nucleolar substrates when compared to its Csm1-binding domain.

Figure 2.6: Ulp2's C-terminal SIM and the Csm1 binding domain have overlapping functions in regulating the desumoylation of the RENT complex *in vivo* (A) Schematic of the quantitative MS analysis used to determine the protein sumoylation levels of ulp2 mutants relative to the wildtype. (B) Average fold increases in sumoylation of Cdc14, Net1 and Tof2 in *ulp2-SIM^{3A}*, *ulp2-F839D* and *ulp2-SIM^{3A}F839D* mutants with respect to the wildtype cells. Average fold increases are quantified based on the average abundance ratio (see Methods for details). (C) Immunoblotting for Net1 in purified sumoylated protein showing maximal desumoylation of Net1 requires both Ulp2 C-terminal SIM and Csm1-binding domain. Schematic of the endogenous sumoylated protein purification by Ni-Flag immunoprecipitation and Western blotting for Net1 shown in right panel; Western blot showing Net1 in wildtype compared to *ulp2-mutants* in whole cell extracts and elutions of the Ni-Flag purification. (D) Schematic showing the mechanism though which Ulp2 orchestrates its substrate specificity toward its nucleolar substrates through its Ulp2 C-terminal SIM and Csm1-binding domain. Maximal desumoylation of its nucleolar substrates associated with the rDNA—Cdc14, Net1 and Tof2—requires both the Ulp2 C-terminal SIM and the Csm1-binding domain.

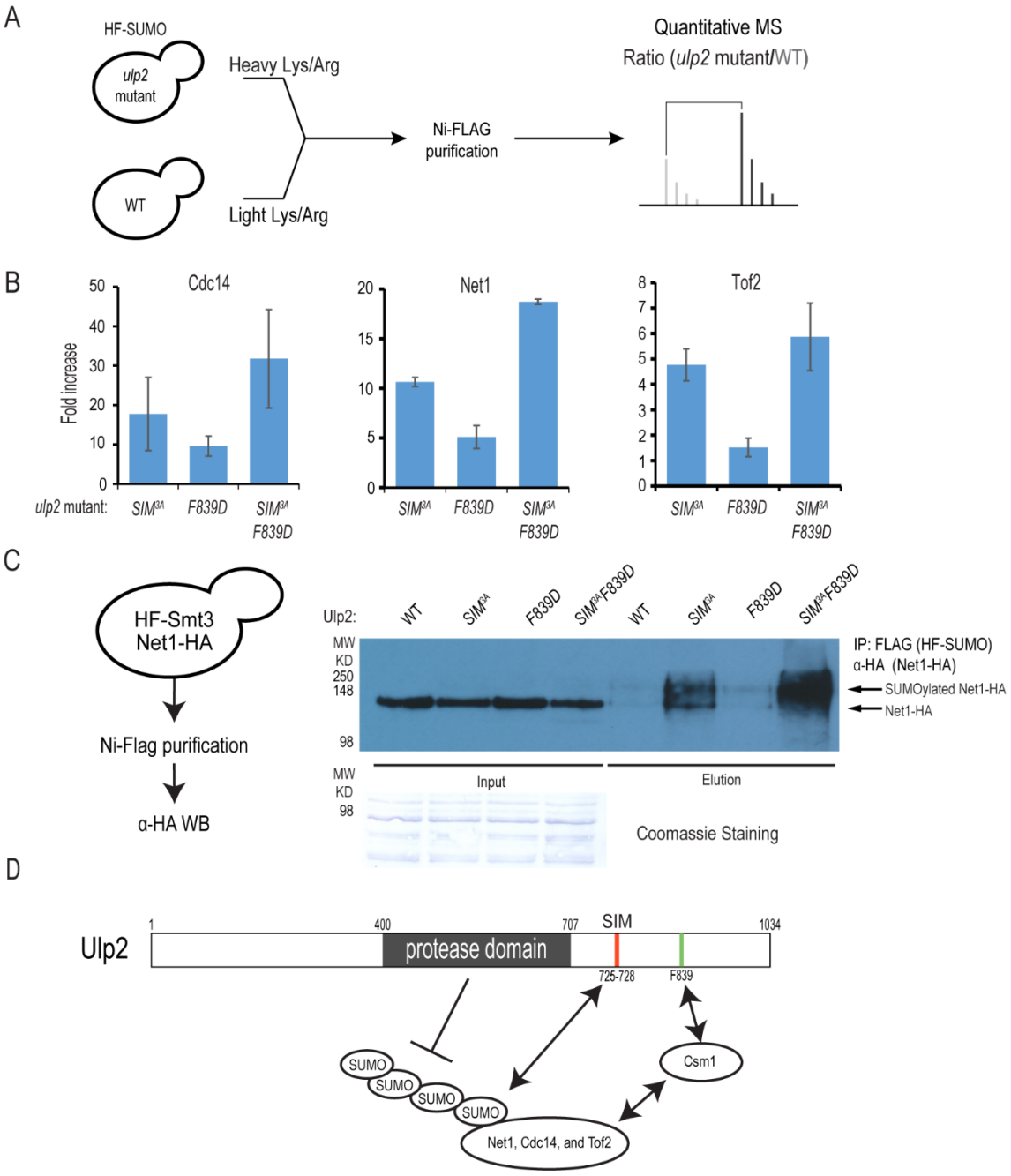
A
HF-SUMO
ulp2 mutant
WT
Heavy Lys/Arg
Light Lys/Arg
Ni-FLAG purification
Quantitative MS
Ratio (ulp2 mutant/WT)
B
Cdc14
Net1
Tof2
Fold increase
ulp2 mutant:
SIM3A
F839D
SIM3A F839D
C
HF-Smt3 Net1-HA
Ni-Flag purification
α-HA WB
Ulp2:
WT
SIM3A
F839D
SIM3AF839D
MW KD
250
148
98
IP: FLAG (HF-SUMO)
α-HA (Net1-HA)
SUMOylated Net1-HA
Net1-HA
Input
Elution
Coomassie Staining
D
Ulp2
1
400
707
SIM
1034
protease domain
725-728
F839
SUMO
Csm1
Net1, Cdc14, and Tof2

2.3 Discussion

Previous findings from growth assays have suggested that the removal of Ulp2's C-terminal domain results in minimal impact on cell growth (Kroetz et al., 2009), contrary to our results (Figure 2.1C). Further research, however, revealed that the *ulp2Δ* mutant is prone to accumulation of survivor mutants and exhibits unique aneuploidy, suppressing its growth defect (Ryu et al., 2016). This tendency of the *ulp2Δ* strain to form survivor mutants is also likely found in *ulp2* C-terminal mutants, masking any growth defect that might be present in each mutant that we tested.

For this reason, we adopted a plasmid loss assay in this study to allow the rapid removal of a complementary *WT ULP2* to reveal the effects of mutating specific C-terminal regions of *ulp2* (Figure 2.1B). Our results show that these specific mutations in *ulp2* C-terminal conserved region do exhibit growth defects which can be severely deleterious to growth when combined. In addition, when these specific C-terminal mutations were integrated to the chromosomal locus, the growth defect was obscured after approximately 100 generations (de Albuquerque, Suhandynata, Carlson, Yuan, & Zhou, 2018), consistent with the conflicting results shown in the previous study (Kroetz et al., 2009). Although it would be interesting to determine whether the previously described aneuploidy defects observed in *ulp2Δ* are also present in these Ulp2 C-terminal mutants, independent lines of evidence consistently support that the three Ulp2 C-terminal conserved regions—SIM, CCR, and Csm1-binding domain—have specific and overlapping functional roles important to cell growth and proliferation.

A well-known characteristic of the SUMO interacting motif is that the SIM-SUMO interaction generally exhibits a weak to modest binding affinity (Song et al., 2004). In agreement with this, the ITC measurement of Ulp2 C-terminal SIM peptide exhibited a modest affinity to both monomeric SUMO and linear SUMO chains with increased binding affinity for longer SUMO chains (Figure 2.2), suggesting that the C-terminal SIM acts to allow more efficient processing of substrates with additional sumoylation through better binding. An *in vitro* SUMO protease assay using recombinant Ulp2$^{400-767}$ provided additional evidence to support this model and demonstrated that the SIM effectively allowed Ulp2$^{400-767}$ to process polySUMO chains when compared to its SIM defective variant Ulp2$^{400-767}$ SIM^{3A} (Figure 2.3 and 2.4). Evidence from *in vivo* data implicated a strikingly strong requirement for the Ulp2 C-terminal SIM in desumoylating its known targets at the nucleolus—Cdc14, Net1 and Tof2 (Figure 2.6D), suggesting that the Ulp2 SIM can function primarily as a means for its recruitment to its highly SUMO-conjugated nucleolar substrates for their subsequent desumoylation. In this case, whether these highly SUMO-conjugated nucleolar substrates recruit Ulp2 via branch polysumoylation or multi-site SUMO conjugation remains to be determined; however, independent data suggest that these highly sumoylated Ulp2-targetted substrates at the nucleolus are conjugated via multi-site SUMO conjugations. First, examatination of a Ulp2 deletion mutant in the 4R-*smt3* background (which lacks the primary N-terminal lysines on SUMO for polySUMO branching) showed that these Ulp2 nucleolar substrates—Net1 Tof2 and Cdc14—can still accumulate at the same level as those substrates in a *ulp2Δ-WT SMT3* background, suggesting that this comparable accumulation of sumoylation caused

by the Ulp2 deletion in both the 4R-*smt3* and wildtype backgrounds is likely due to SUMO conjugation at several different sites on these nucleolar substrates (de Albuquerque et al., 2016). In agreement with this multi-site conjugation model, MS results identified that multiple lysines on both Net1 and Tof2 are sumoylated, although a complete mapping of their SUMO sites remains incomplete (Albuquerque et al., 2015).

An important question arises when considering Ulp2's ability to bind to SUMO via its C-terminal SIM: why does Ulp2 only desumoylate these relatively few substrates, while Ulp1 acts to desumoylate the vast majority of sumoylated proteins in the cell? There are several possible explanations for why Ulp2 only targets these relatively fewer and specific substrates when compared to Ulp1. The first underlying clue may be the relatively different binding affinities of these proteins to SUMO. Results from prior studies using binding kinetic assays demonstrate that the Ulp1 catalytic domain can bind to SUMO extremely well with nanomolar affinity (K_d = 12.9nM) (Elmore et al., 2011). In contrast, SUMO binding to the Ulp2 catalytic domain, or its human ortholog *SENP7*, has not been previously described (Lima & Reverter, 2008) or detected in our own binding assays (Unpublished results).

Although Ulp1 performs the majority of the desumoylation within the cell and displays strong binding to SUMO and catalysis of sumoylated substrates (de Albuquerque et al., 2016; Li & Hochstrasser, 1999), Ulp1 is unable to desumoylate Ulp2-targetted substrates. Previous work has shown that Ulp1 displays distinct localization at the nuclear periphery (Li & Hochstrasser, 2003; Panse, Kuster, Gerstberger, & Hurt, 2003) and is absent in the nucleolus (Zhao, Wu, & Blobel,

2004). Consistent with this notion, mis-localization of Ulp1 by deletion of the localization signal at its N-terminus results in aberrant desumoylation of Ulp2 specific substrates (de Albuquerque et al., 2016), and has been shown to result in diffusion of Ulp1 throughout the cell (Li & Hochstrasser, 2003; Panse et al., 2003). These observations together support the theory that the potent activity of Ulp1 is perhaps restricted to the nuclear periphery, making Ulp1 inaccessible to those Ulp2-specific substrates.

We hypothesize that the modest SUMO binding affinity of Ulp2's C-terminal SIM may act to target those substrates with multiple SUMO conjugations, given the increasing affinity of Ulp2 toward substrates with a greater number of SUMO conjugations. Ulp2 has been shown to localize throughout the nucleoplasm; however, it is known to be recruited to the rDNA locus through its association with the cohibin complex Csm1:Lrs4 via its C-terminal Csm1 binding domain (Liang et al., 2017; Srikumar et al., 2013). Cdc14, Net1 and Tof2 have been shown to form large protein complexes as part of the rDNA maintenance network (Huang & Moazed, 2003), many components of which are known to be sumoylated (Gillies et al., 2016). This observation suggests that there may be a mechanism by which cells could continuously sumoylate these rDNA-associated substrates—Cdc14, Net1 and Tof2—and once sumoylation reaches a certain level that is sufficient to recruit Ulp2 via its C-terminal SIM, their SUMO conjugations could then be efficiently downregulated by Ulp2. Although other nucleolar proteins are also known to be sumoylated, including Rpa135 and Rpa190 (de Albuquerque et al., 2016), their sumoylation doesn't appear to be affected by the deletion of Ulp2. One possible

explanation is that they are not highly sumoylated compared toCdc14, Net1 and Tof2, which likely are continuously being sumoylated. It is relevant to note here that the aberrant desumoylation of Cdc14, Net1 and Tof2 caused by mislocalized Ulp1 does not affect other sumoylated nucleolar proteins, including Rpa135 and Rpa190 (de Albuquerque et al., 2016). Collectively, these results suggest that Ulp2 orchestrates its specificity toward its nucleolar substrates through: (1) Ulp2's recruitment to the nucleolus via its Csm1 binding domain, and (2) targeting those highly sumoylated nucleolar proteins—Cdc14, Net1 and Tof2—via its C-terminal SIM (Figure 2.6D).

Other than the nucleolar substrates described above, Ulp2 has been shown to also specifically desumoylate several proteins of the inner kinetochore complexes and specific subunits of the MCM complex (de Albuquerque et al., 2016). We speculate that the mechanism by which Ulp2 targets these subunits is analogous to how it targets its nucleolar substrates, involving a protein-protein interaction that recruits nearby Ulp2 and leverages this spatial proximity to allows the Ulp2 C-terminal SIM to recognize those subunits that are hyper-sumoylated. In support of this notion, mutations that eliminate Ulp2-Csm1 binding do not appear to lead to a drastic increase in sumoylation in either kinetochore or MCM subunits compared to deletion of Ulp2 (Liang et al., 2017). This observation suggests that Csm1 binding does not play a role in targeting these two groups of Ulp2-specific substrates. Moreover, mutations in the three C-terminal conserved regions of Ulp2 revealed that the cells require CCR for optimal cell growth in addition to the Csm1-binding domain and Ulp2 C-terminal SIM (Figure 2.1C), and it is particularly necessary when

mutations in these regions are combined. This suggests that CCR may play an important role in mediating other functions of Ulp2, but further studies are needed to fully understand how Ulp2 coordinates its substrate specificity and to determine the role of CCR in mediation of Ulp2 function.

2.4 Methods

Yeast strain construction and plasmid construction

Standard yeast genetics techniques were used in the construction of the yeast strains, and the genotypes of all strains and plasmid used in this study can be found in table A2 in appendix. Deletion of Ulp2 was performed by gene disruption by the insertion of NatMX4 at the *ULP2* chromosomal locus using polymerase chain reaction (PCR)-based methods and selection with nourseothricin. To ensure the removal of the wildtype allele, all deletions were confirmed by DNA sequencing. The plasmids used in the 5-FOA sensitivity assay were constructed as follows: the seven different *ulp2*- alleles containing mutations in their C-terminal conserved domains (*ulp2- SIM^{3A}, F839D and CCR^{3A}*) and a wildtype *ULP2* (control) were placed on a pRS315 plasmid with a C-terminal 6xHis-3xFlag-Protein A (TAF) tag.

Plasmid for the Mature Smt3 (SUMO) was cloned into the pET21B vector with an N-terminal 6xHis tag allowing for the expression and purification of SUMO monomer. Other constructs used to express the recombinant linear SUMO chains (2x-SUMO, 4x-SUMO and 6x-SUMO) contain an additional TEV (Tobacco Etch Virus) Protease cleavage site between the N-terminal 6xHis tag and the linear SUMOs and were a generous gift from Dr. Kevin D. Corbett (UCSD). Ulp2$^{400\text{-}767}$ Wildtype and SIM-3A variants (Ulp2$^{400\text{-}767}$ WT and Ulp2$^{400\text{-}767}$ SIM^{3A}) were cloned into 2BT LIC vector (pET 6xHis TEV LIC cloning vector), which also contains a N-terminal 6xHis-tag followed by a TEV protease site.

5-FOA sensitivity assay

The 5-FOA sensitivity assay was performed as follows: the eight different *ulp2*-alleles placed on pRS315 plasmids were transformed into HZY3658 which carries the complementing wildtype *ULP2* on a pRS316 plasmid. These strains were first cultured to late log-phase (OD600 ~ 2.0) in Complete Synthetic Medium lacking leucine (0.69 g/L CSM –Leu drop out mix, 7 g/L Yeast Nitrogen Base and 20 g/L glucose) and were normalized by optical density (OD600) to ensure equal plating.

Five 1:10 serial dilutions were performed to the normalized cultures using sterile deionized water in a sterile 96 well plate and then 4µL of each dilution was spotted onto either YPD (1.0% Yeast extract, 2.0% Peptone, 2% D-glucose and 2.4% agar) or 5-Fluoroorotic Acid (0.67% yeast nitrogen base, 0.77 g/L CSM –Ura drop-out mix, 20 mg/L uracil 0.1% 5-FOA plates and 2.4% agar). Both YPD and the 5-Fluoroorotic Acid plates were incubated for 2-5 days at 30°C, and imaged using a Bio-Rad ChemiDocTM MP imaging system.

Abundance of Ulp2 in ulp2 C-terminal Conserved domain mutant strains

To evaluate the relative abundance of Ulp2 in each of the strains analyzed in the 5-FOA sensitivity assay, eight strains taken from the 5-FOA plates were first grown to log-phase (OD600 at 0.5) in 50mL YPD cultures. The yeast whole cell extracts (WCE) were prepared by a base-acid lysis method described below and analyzed by immunoblotting for TAP-tagged Ulp2 using α-Protein A primary antibody (Sigma P3775) and α-rabbit-HRP secondary antibody (Millipore Sigma). Equal amounts were also analyzed by Coomassie staining of a SDS-PAGE gel as a loading control.

The base-acid lysis method used to generate WCE was performed by the addition of 250μL of glass beads, 200μL of 1M NaOH, 500μL of H2O, 100μL of 1M phosphate buffer (pH8.0) and 200μL of 10% Sodium Dodecyl Sulfate (SDS) to the pelleted cells which were then lysed by vortexing at 4ºC for 5 min. The lysed cells were then neutralized by the addition of 200 μL of 1M HCL and heated at 65ºC for 10 min prior to centrifugation.

Cell Cycle Analysis of Ulp2 in ulp2 C-terminal conserved domain mutant strains

Cell cycle profiles of the strains analyzed in the 5-FOA sensitivity assay were performed by flow cytometry (FACS analysis). 300 μL log-phase cultures (0.5 OD600) were fixed in 70% ethanol, and digested with RNase A (250μg/mL) and Proteinase K (1 mg/mL) in 50mM Sodium Citrate pH 7.0 overnight at 37 ºC. Digested samples were then resuspended by sonication (VWR Branson 450) in 1mL of 50mM Sodium Citrate pH7.0 and 1μM Sytox Green (Genscript) and incubated in the dark for 30 minutes prior to analysis by flow cytometry (BD LSR II flow cytometer).

SUMO binding assay

To detect binding between Ulp2 C-terminal conserved regions and SUMO, biotinylated peptides of Ulp2 C-terminal SIM, CCR and their 3A-variants were bound to 10 μL NeutrAvidin agarose resin and incubated with linear SUMO mixtures containing 20 μg of each of the linear SUMO constructs (1xSUMO, 2SUMO, 4xSUMO and 6xSUMO) in 100 μL of Phosphate Saline Buffer at 4ºC for 2 hours.

The resins were then washed 3 times with 200 μL phosphate saline buffer. Elution was performed by incubating the resin with 100 μL of 2% SDS at 98ºC for 5 min. 5% of the binding reaction eluents, input and flow-through were analyzed using a 15% SDS-PAGE gel and visualized by Coomassie staining. The biotinylated peptides of Ulp2 C-terminal SIM, CCR and their 3A-variants were purchased from EZbio with the following amino acid sequence: Ulp2 $^{708\text{-}743}$ SIM: Biotin-KSTNINNNENYDDDDEEIQIIENIDQSSKDNNAQLT; Ulp2 $^{708\text{-}743}$ SIM^{3A}: Biotin-KSTNINNNENYDDDDEEAQAAENIDQSSKDNNAQLT; Ulp2 $^{896\text{-}937}$ CCR: Biotin-NNTNIVISDTEQDSRLGVNSESKNTSGIVNRDDSDVNLIGSS; Ulp2$^{896\text{-}937}$CCR^{3A}: Biotin-NNTNIVISDTEQDSRLGVNSESKNTSGIVNRDDSDANAAGSS.

Isothermal calorimetry (ITC)

ITC experiments were performed by Sanford Burnham Prebys Medical Discovery Institute Protein Analysis Core Facility using an ITC200 calorimeter from Microcal (Northampton, MA). In the ITC experiments performed, 19 increments of 2.0 μl of 2 mM Ulp2 C-terminal SIM peptide (DDDDEEIQIIENIDQSSKD, Genscript) were titrated into the device cell containing each of the linear SUMO chain constructs (1xSUMO, 4xSUMO and 6xSUMO) at 23ºC. A total of two replicates of each ITC experiment was performed, and the ITC data was analyzed with Origin software provided by Microcal.

Protein expression and purifications

Each of the four linear SUMO chain constructs (1xSUMO, 2xSUMO, 4xSUMO and 6xSUMO) were transformed into *E. coli* RosettaTM-2(DE3)pLysS cells and grown in 4 liters of LB (Luria Broth) media with 100 µg/mL of ampicillin at 37ºC until optical density reached 0.6 OD600. Induction was performed by the addition of isopropyl β–D-1-thiogalactopyranoside (IPTG) with a final concentration of 0.2mM and incubated overnight at 18 ºC. The pelleted cells containing each of the constructs were lysed in phosphate buffered saline (PBS) with 10% glycerol and 14 mM β-Mecaptoethanol (βME) by sonication (VWR Branson 450). These constructs were purified first using nickel nitrilotriacetic acid resin (Ni-NTA) (Qiagen) columns and followed by FPLC gel filtration (Superdex 200 10/300 GL) using an ÄKTA pure FPLC system. Fractions containing purified constructs were pooled and stored in -80 ºC. The $Ulp2^{400-767}$ Wildtype and SIM-3A variants ($Ulp2^{400-767}$ WT and $Ulp2^{400-767}$ SIM^{3A}) were also expressed and lysed as described. Constructs containing $Ulp2^{400-767}$ Wildtype and SIM-3A variants were purified by first using nickel nitrilotriacetic acid resin (Ni-NTA) (Qiagen) columns and followed by cation exchange (HiTrap SP), gel filtration (Superdex 200 10/300 GL) and anion exchange (monoQ 5/50 GL) using an ÄKTA pure FPLC system. Aos1-Uba2 (E1), Ubc9 (E2), and Siz1 (E3, residues 167-465) enzymes were expressed in *E.coli* RosettaTM-2(DE3)pLysS cells were purified by affinity chromatography as described in (Albuquerque et al., 2015).

Synthesis of in vitro polySUMO chains

Poly-SUMO chains were generated via *in vitro* sumoylation reactions using mature Smt3 (5 μM SUMO) and recombinant E1, E2 and E3 enzymes: 0.4 μM Aos1-Uba2 (E1), 2 μM Ubc9 (E2), and 0.4 mM Siz1 (E3, residues 167-465); in 20 mM HEPES pH7.5, 0.15 M NaCl, 1 mM ATP, and 2 mM MgCl2. Reactions were quenched after a 1 hour incubation at 30 °C by the addition of EDTA to a final concentration of 100mM.

SUMO protease assay

The SUMO protease assays on the linear SUMO constructs were performed *in vitro* the addition of 1ug of $Ulp2^{400-767}$ WT or $Ulp2^{400-767}$ SIM^{3A} to 100 μg of each construct (1xSUMO, 2xSUMO, 4xSUMO and 6xSUMO) at room temperature in 50 μL of PBS with 1 mM dithiothreitol. 5 μL aliquots of each reactions were collected in 45 μL LDS buffer at 0, 15, 30, and 60 min. 10 μL of the LDS samples (2% reaction equivalent; 2 μg equivalent of linear SUMO) for each time point were analyzed by 15% SDS-PAGE gel and visualized with Coomassie staining. Densitometry analysis was performed by using ImageJ software.

Peptide inhibition of the SUMO protease assay of $Ulp2^{400-767}$ WT on the 6x-SUMO was performed as described with the addition SIM peptide (Biotin-KSTNINNNENYDDDDEEIQIIENIDQSSKDNNAQLT) at various concentrations (720, 360, 180, 90 and 45 μM). Results from one time point (60 min.) of each reaction are shown in Figure 4A, while results from all time points (0, 15, 30, and 60 min) of the

SUMO protease assay with 360 μM SIM peptide and no peptide are shown in Figure 4B.

The SUMO protease assays on the *in vitro* synthesized polySUMO were performed as described with the following modification: 0.75 μg of Ulp2$^{400-767}$ WT or Ulp2$^{400-767}$ SIM^{3A} was used for 75 μg *in vitro* synthesized polySUMO, and 0.04% reaction equivalent (30 ng equivalent of linear SUMO) was loaded on 4-12% gradient gels (Invitrogen) and analyzed by immunoblotting for Smt3 with rabbit polyclonal Ab α-Smt3 (in house) and a α-rabbit-HRP secondary antibody (Millipore Sigma).

Affinity purification of endogenous sumoylated proteins

HF-*SMT3 ulp2Δ* NET1-HA (HZY3725) cells were grown in 2L of YPD and harvested in late-log phase (OD600 at 1.5). Harvested cells were washed with PBS-NP40 (0.2% NP-40) containing 10 mM Iodoacetamide and 10 mM N-ethyl maleimide (NEM) and protease inhibitor cocktail (2 mM phenylmethylsulfonyl fluoride, 200 μM benzamidine, 0.5 μg/mL leupeptin, 1 μg/mL pepstatin A) before being resuspended to a final volume of 2.5mL. Resuspended cells were frozen dropwise in liquid nitrogen and lysed by pulverization using a SPEX SamplePrep 6875D freezer/mill. PBS-NP40 (¼-volume equivalent) with protease inhibitor cocktail was added to thaw the cells and the thawed lysate was clarified by ultracentrifugation.

Endogenous sumoylated proteins were bound to 100μL of anti-FLAG-M2 resin (SIGMA) for 2 hours at 4ºC. The resin was washed 4 times with 2 mL of PBS-NP40 containing protease inhibitor cocktail. Endogenous sumoylated proteins were eluted

with 1000 µL of PBS containing 10% glycerol, 12 mM βME, 0.2 mg/mL 3x-Flag peptide and protease inhibitor cocktail.

Quantitative MS analysis

The quantitative MS analysis used in evaluating changes in sumoylation between wildtype cells and each of the *ulp2* C-terminal conserved region mutants (*ulp2-SIM^{3A}, ulp2-F839D, and, ulp2-SIM^{3A}F839D*) was performed as described in Albuquerque et al., 2018 (de Albuquerque et al., 2018).

2.5 Acknowledgements

Chapter 2, in part, contains material as it appears in de Albuquerque, Suhandynata, Carlson, Yuan, & Zhou, 2018.

Section 2.2.1 describes a growth analysis a growth analysis and experiments addressing the Ulp2 protein abundance and the cell cycle profile of *ulp2* C-terminal mutants that were designed and performed by Dr. Raymond T. Suhandynata.

In Section 2.2.3, the competitive inhibition of SUMO protease activity by SIM peptide described section was designed and performed by Dr. Claudio ponte de Albuquerque.

In Section 2.2.4, the SUMO protease assay on *in vitro* generated polySUMO that was designed by Dr. Claudio ponte de Albuquerque, and the purification of endogenous sumoylated protein and the SUMO protease assay on endogenous sumoylated protein described in this section were designed and performed by Dr. Claudio ponte de Albuquerque.

Section 2.2.5 describes MS experiments designed performed and analyzed by Dr. Claudio ponte de Albuquerque and Dr. Raymond T. Suhandynata.

I would like to thank members of Zhou lab and the previous works that made this publication possible.

Chapter 2, in part, contains material as it appears in Binding to small ubiquitin-like modifier and the nucleolar protein Csm1 regulates substrate specificity of the Ulp2 protease 2018. de Albuquerque, C. P.; Suhandynata, R. T.; Carlson, C. R.; Yuan, W. T.; Zhou, H., J Biol Chem, 2018.

Chapter 3:

Catalytic inactive Ulp1 protease domain—Ulp1$^{403-621}$ C580S—can be used to purify endogenous total sumoylated protein

3.1 Introduction

In the previous chapter, we evaluated the sumoylation status three known Ulp2 nucleolar substrates—Cdc14, Net1, and Tof2—in strains with mutations in the Ulp2 C-terminal conserved region, and demonstrated that Ulp2's C-terminal SIM and its Csm1 binding domain collectively promote desumoylation of its nucleolar substrates. This approach required the use of affinity or epitope tagged SUMO strains (HF-SUMO), which allow for the purification of total endogenous sumoylated protein for subsequent biochemical analysis. One concern with this approach is that tagging SUMOs in the cell appears to compromise polySUMO formation to a certain extent (de Albuquerque et al., 2016). Genetic evidence supporting this observation can be seen in *ulp2* deletion strains expressing either 6xHIS-3xFLAG-Smt3 (HF-SUMO) or HF-4R-SUMO (SUMO with four lysine-to-arginine mutations at its major N-terminal SUMO-SUMO linkages) (de Albuquerque et al., 2016). In both cases, the specific *ulp2* deletion defects, including slow growth and excessive accumulation of polysumoylated proteins (Bylebyl et al., 2003), appears to be partially alleviated. Since HF-SUMO may partially compromise formation of polysumoylation, it is conceivable that hyper sumoylation in a *ulp2* deletion background may also be compromised. This is concerning, as results from studies that have investigated the functional consequence of elevated sumoylation may have been affected through use of N-terminal SUMO tags. Thus, the ideal method to obtain a more accurate profile of Ulp2-dependent targets would be to adopt an approach that bypasses the need to use HF-SUMO.

Possible ways to address this issue include utilization of reagents that can bind to SUMO and sumoylated substrates with sufficient affinity as a purification reagent. Structural analysis of the Ulp1 protease domain and SUMO as published by Mossessova and Lima revealed that the entire Ulp1 protease domain binds to SUMO extensively and provided the first characterization of the residues responsible for catalysis (Cys580, His514, and Asp-531) (Mossessova & Lima, 2000). Building upon these findings, later studies showed that a catalytically inactive Ulp1 protease domain, $Ulp1^{403-621}$ C580S, binds to sumo with nanomolar affinity (K_d =12.9nM) (Elmore et al., 2011). In addition, this study demonstrated that the $Ulp1^{403-621}$ C580S construct can be used to purify endogenous sumoylated protein and would abrogate the need to use HF-SUMO to purify endogenous sumoylated protein.

In this chapter, we further investigated the mechanism by which Ulp2 targets its substrates at the kinetochore. Building upon our study of the Ulp2 SIM, we developed use of Sepharose-conjugated $Ulp1^{403-621}$ C580S (dUlp1) to purify endogenous sumoylated proteins from non-HF-tagged SUMO cells, particularly focusing on the kinetochore subunits that Ulp2 is also known to target in order to assess whether the Ulp2 CCR acts in a similar manner to the rDNA targeting region of Ulp2, itsCsm1-binding domain.

3.2 Results

3.2.1 Resin conjugated catalytic inactive Ulp1 protease domain—Ulp1$^{403-621}$ C580S—can be used to purify endogenous total sumoylated protein

Given that the catalytically inactive Ulp1 had been shown to bind to SUMO with nanomolar affinity (Elmore et al., 2011), we asked whether the recombinantly expressed and purified catalytically inactive Ulp1 catalytic domain—Ulp1$^{403-621}$C580S —can be used as an alternative reagent to purify sumoylated proteins. In our construct, we tagged the Ulp1$^{403-621}$C580S with an N-terminal 6xHis-MBP-tag (Figure 3.1A) and we referred to the N-terminal tagged 6xHis-MBP Ulp1$^{403-621}$C580S construct as dUlp1.

The dUlp1 was overexpressed and purified from bacteria by Ni affinity purification. The overexpressed bacterial whole cell lysate, the Ni-affinity purification flow through and the elution fractions were analyzed by SDS-Page and visualized by Coomassie staining (Figure 3.1C). The elution fractions containing the dUlp1 after one step Ni affinity purification showed minimal contaminants, and thus these fractions were combined and dialyzed prior to immobilization.

The purified dUlp1 was then immobilized through chemical conjugation to cyanogen bromide-activated Sepharose. The conjugation reaction was evaluated by analyzing equal amounts of the input and flow through by SDS-Page and visualized by Coomassie staining (Figure 3.1D). Almost no intensity could be detected at the corresponding molecular weight of dUlp1 in the flow-through sample, and this shows that nearly all the dUlp1 was conjugated to the Sepharose resin.

To evaluate whether dUlp1 resin could purify endogenous sumoylated proteins, resin-bound dUlp1 was incubated with yeast protein extracts from a *WT SMT3*

strain. After incubation, the resin bound dUlp1 was washed repeatedly, and was then eluted by the addition of SDS-Page buffer with 1xSDS and boiled for 5 minutes. The input and flow-through after incubation were analyzed together with the eluent by anti-Smt3 immunoblot (Figure 3.1E), and the blot was subsequently stained with Coomassie as loading control. By incubating the yeast whole cell lysate with the immobilized dUlp1, the total sumoylated protein was depleted as shown through comparison between the flow-through and input sample in Figure 3.1E. In the elution sample, the total sumoylated protein appears to be significantly enriched, showing that total sumoylated protein was purified.

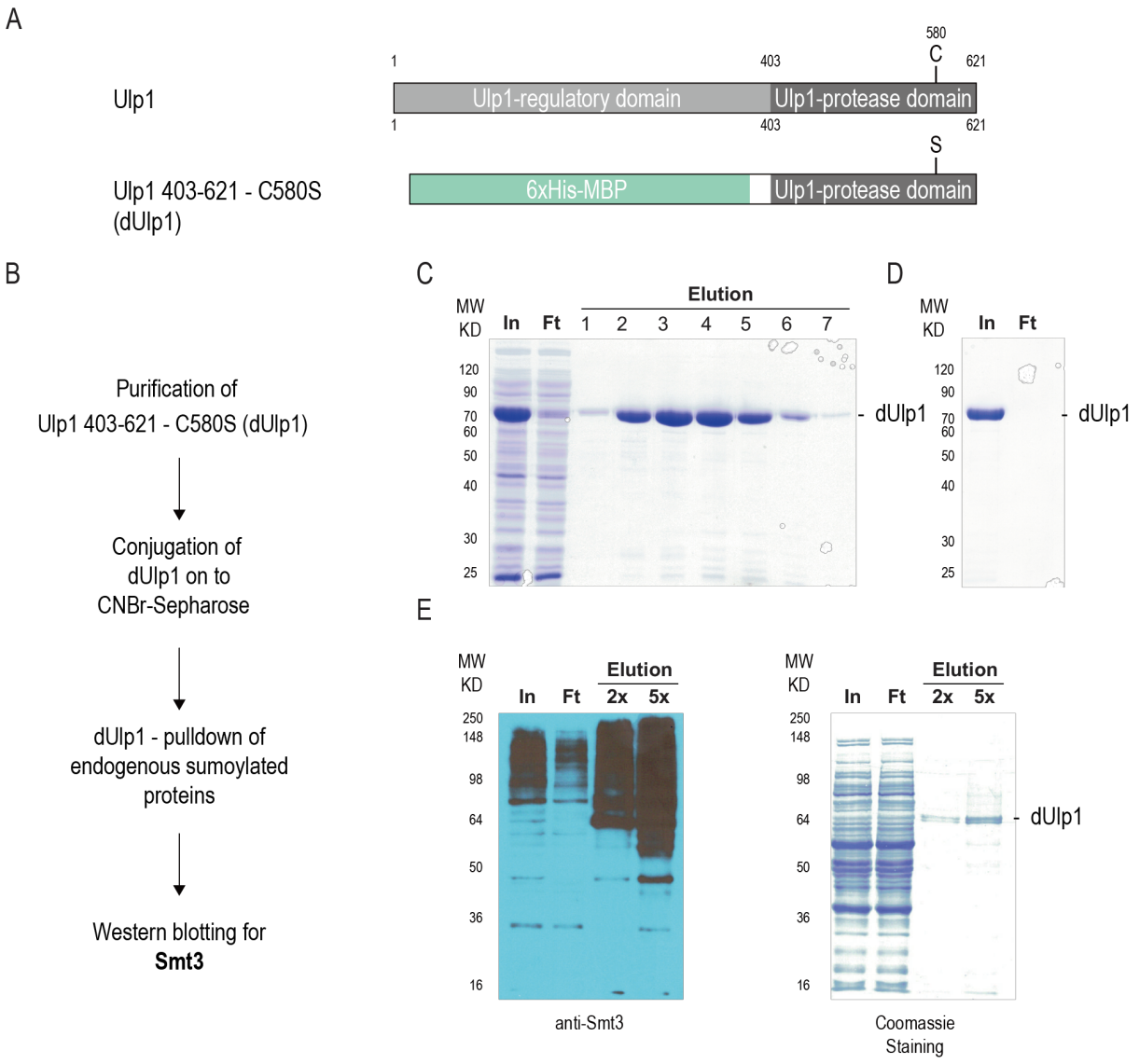

Figure 3.1: Resin conjugated catalytic inactive Ulp1 protease domain—Ulp1$^{403-621}$ C580S—can be used to purify endogenous total sumoylated protein (A) Construct of the catalytically dead Ulp1 protease domain (dUlp1) in comparison to the wildtype full-length Ulp1 SUMO protease. (B) Flowchart outlining the development and use of the dUlp1-pulldown for the purification of endogenous sumoylated protein. (C) Ni-affinity purification of recombinantly expressed dUlp1 protein from IPTG-induced Rosetta (DE3) E. coli whole cell lysate. (D) Conjugation reaction of dUlp1 to Cyanogen-activated Sepharose resin. (E) Western blot showing purified endogenous sumoylated protein by dUlp1 pulldown in wildtype SUMO strains. Loading controls are shown by Coomassie staining.

3.3 Discussion

One of the most challenging factors in the biochemical analysis of sumoylated protein is posed by the low abundance of sumoylated substrates relative to their unconjugated forms. In many studies, including many experiments in Chapter 2, an affinity tag-SUMO is used and serves mainly to purify endogenous sumoylated protein (Andersen, Matic, & Vertegaal, 2009; Munk et al., 2017; Wykoff & O'Shea, 2005). However, as previously mentioned, tagging SUMO may partially compromise polySUMO formation *in vivo* (de Albuquerque et al., 2016). This poses a significant concern when the subject of investigation is polysumoylated or involved in polysumoylation, such as Ulp2, which is known to suppress sumoylated polySUMO *in vivo* (Bylebyl et al., 2003).. This complication prompted the search for an alternative way to purify endogenous sumoylated protein without tagging SUMO. In this chapter, we show that the immobilized catalytically inactive Ulp1 catalytic domain (dUlp1), 6xHis-MBP Ulp1$^{403-621}$C580S, can be used as a reagent to purify endogenous sumoylated protein from yeast whole cell lysate.

The potent SUMO protease activity of Ulp1 id likely is due to the mechanism through which the Ulp1 protease domain binds to SUMO. In the Ulp1-SUMO co-crystal structure solved by Mossessova and Lima, the SUMO C-terminal extension has been shown to enter a shallow but constricted hydrophobic tunnel of Ulp1 (Mossessova & Lima, 2000). While this tunnel appears to interact extensively with SUMO C-terminal di-glycine, the Ulp1 residue W448, which is responsible for closing this hydrophobic pocket onto the di-glycine, exposes a substantial area immediately adjacent to the end of the C-terminal SUMO carboxylate (Reverter & Lima, 2004).

This structure likely explains Ulp1's ability to hydrolyze both the SUMO C-terminal extension (-ATY) peptide bond in SUMO precursor and its ability to cut various large SUMO adducts (Li & Hochstrasser, 2003; Mossessova & Lima, 2000). Thus, the catalytically inactive form of Ulp1, which had been shown to bind to SUMO with nanomolar affinity (Elmore et al., 2011) *in vitro*, likely binds to all sumoylated proteins, including polysumoylated protein. Consistently, the *ulp1-N338Δ* mutation, which has been shown to compromise localization of Ulp1 to the Nuclear Pore Complex, causes Ulp1 to desumoylate the Ulp2-dependent substrates that are normally hyper-sumoylated (de Albuquerque et al., 2016). Collectively, these results suggest that dUlp1 should bind to SUMO as well as sumoylated and polysumoylated substrates indiscriminately; however, further testing is needed to confirm that the ability of dUlp1 to bind to various adducts is comparable.

3.4 Methods

Plasmid construction and protein purification

The Ulp1$^{403-621}$C580S was placed in pET 6xHis-MBP Asn_{10} TEV LIC (Ligation independent cloning) vectors by Gibson assembly and was transformed into *E. coli* RosettaTM-2(DE3)pLysS cells. Cells were grown in 2 liters of LB (Luria Broth) media with 100 µg/mL of ampicillin at 37ºC until optical density reached 0.6 OD600. Induction was performed by the addition of isopropyl β–D-1-thiogalactopyranoside (IPTG) with a final concentration of 0.2mM and incubated overnight at 18 ºC. The pelleted cells containing 6xHis-MBP-Ulp1$^{403-621}$C580S were lysed in phosphate buffered saline (PBS) with 10% glycerol and lysed by sonication (VWR Branson 450). The 6xHis-MBP-Ulp1$^{403-621}$C580S was purified by 5mL HisTrap HP column (GE Healthcare) using an ÄKTA pure FPLC system. Fractions containing 6xHis-MBP-Ulp1$^{403-621}$C580S were pooled and dialyzed with phosphate buffered saline (PBS).

Immobilization of the Ulp1$^{403-621}$C580S

The dialyzed Ulp1$^{403-621}$C580S was incubated with CNBr- activated Sepharose that was pre-washed with 100 mL of 1mM HCL for 1 hours in 4ºC. After binding, the immobilized Ulp1$^{403-621}$C580S Sepharose was washed with 5 medium volumes of 100mM Tris-HCl (pH8), 300mM NaCl, and stored in PBS with 55% glycerol at -20ºC.

Purification of endogenous sumoylated protein by dUlp1 pulldown

HZY3658 (MAT a, *ulp2Δ::natMX4*, pRS316-*ULP2,* W303) cells were grown in 100mL of YPD and harvested in log phase (OD600 at 1.0). Harvested cells were washed twice with PBS-NP40 (0.2% NP-40) containing 20 mM Iodoacetamide and 20 mM N-ethyl maleimide (NEM) and protease inhibitor cocktail (2 mM phenylmethylsulfonyl fluoride, 200 µM benzamidine, 0.5 µg/mL leupeptin, 1 µg/mL pepstatin A) before pelleting by centrifugation into 2mL screw-cap microcentrifuge tubes. The pelleted cells were then stored at -80ºC.

The frozen cell pellet was lysed by mechanical disruption using a Disruptor Genie (SI-D238) with addition of Silica glass beads (0.2mm) and PBS-NP40 with protease inhibitor cocktail at 4ºC. The whole cell lysate was clarified by centrifugation, and then bound to 20µL of resin-bound dUlp1 for 2 hours at 4ºC. The resin was washed 6 times with 1 mL of PBS-NP40 containing protease inhibitor cocktail. The endogenous sumoylated proteins were eluted by the addition of 80µL of 1xLDS and boiled at 98ºC for 5 min.

Input and flow-through of the purification of endogenous sumoylated protein were loaded together with 2x- and 5x-equivalent of the elution onto 10% SDS-Page gels and analyzed by immunoblotting for Smt3 with rabbit polyclonal Ab α-Smt3 (in house) and a α-rabbit-HRP secondary antibody (Millipore Sigma).

3.5 Acknowledgement

Dr. Huilin Zhou designed the approach to use catalytically inactive Ulp1 to purify sumoylated protein from whole cell extracts (Section 3.2.1).

Appendix

A.1 Individual Contributions

My preliminary results were the first to show that Ulp2 C-terminal SIM is needed for Ulp2$^{400-767}$ to efficiently process linear SUMO chains *in vitro*.

In section 2.2.3 and 2.2.4, I expressed and purified the enzymes and substrates used in the SUMO protease assay; specifically, the purification of Ulp2$^{400-767}$, the purification of linear SUMO chains and the generation of *in vitro* polySUMO chains. Furthermore, I performed and quantified the proteases assays using linear SUMO and polySUMO chains.

In section 3.2.1, I expressed and purified the catalytically inactive Ulp1 protease domain, Ulp1$^{403-621}$ C580S. Furthermore, I generated the Sepharose conjugated catalytically inactive Ulp1 protease domain and performed pulldown of sumoylated protein using this resin from yeast whole cell extracts.

A.2 Yeast strain and plasmids used in this study

STRAIN NAME	GENOTYPE	SOURCE
HZY3658	MAT a, *ulp2Δ::natMX4*, pRS316-*ULP2,* W303	Albuquerque, et al, *JBC* 2018
HZY2101	MAT a, *HF-SMT3 sml1Δ::TRP1 arg4Δ ura3-52 leu2Δ1 trp1Δ63 his3Δ200 lys2ΔBgl hom3-10 ade2Δ ade8*.	Albuquerque, et al, PLoS genetics 2013
HZY3676	MAT a, *NET1-HH::HIS3 HF-SMT3,* isogenic to HZY2101	Albuquerque, et al, *JBC* 2018

HZY3678	MAT a, *NET1-HH::HIS3 ulp2-SIM^{3A}::kanMX6 HF-SMT3,* derived from HZY3676	Albuquerque, et al, *JBC* 2018
HZY3679	MAT a, *NET1-HH::HIS3 ulp2-F839D:: kanMX6 HF-SMT3,* derived from HZY3676	Albuquerque, et al, *JBC* 2018
HZY3680	MAT a, *NET1-HH::HIS3 ulp2-SIM^{3A}F839D:: kanMX6, HF-SMT3,* derived from HZY3676	Albuquerque, et al, *JBC* 2018
HZY3973	MAT a, *Ulp2-TAF:: kanMX6 HF-SMT3,* derived from HZY2101	Albuquerque, et al, *JBC* 2018
HZY3963	MAT a, *ulp2-SIM^{3A}-TAF:: kanMX6 HF-SMT3,* derived from HZY2101	Albuquerque, et al, *JBC* 2018
HZY3966	MAT a, *ulp2-F839D-TAF:: kanMX6 HF-SMT3,* derived from HZY2101	Albuquerque, et al, *JBC* 2018
HZY3983	MAT a, *ulp2-SIM^{3A}F839D-TAF:: kanMX6 HF-SMT3,* derived from HZY2101	Albuquerque, et al, *JBC* 2018
HZY621	MAT**a**; *RDN1-NTS1::mURA3 ade2-1 can1-100 his3-11,15 leu2-3,112 trp1-1 ura3-1 RAD5+ cir0(2µm removed), also known as JLY1096*	Liang et al. Genes & Dev. 2017
HZY001	*ulp2-SIM^{3A}::kanMX6, derived from HZY621*	Albuquerque, et al, *JBC* 2018
HZY002	*ulp2-CCR^{3A}::kanMX6, derived from HZY621*	Albuquerque, et al, *JBC* 2018
HZY035	*ulp2-F839D::kanMX6, derived from HZY621*	Albuquerque, et al, *JBC* 2018
HZY003	*ulp2-SIM^{3A}, F839D::kanMX6, derived from HZY621*	Albuquerque, et al, *JBC* 2018
HZY004	*ulp2-F839D, CCR^{3A}::kanMX6, derived from HZY621*	Albuquerque, et al, *JBC* 2018

HZY005	*ulp2-SIM^{3A}, CCR^{3A}::kanMX6, derived from HZY621*	Albuquerque, et al, *JBC* 2018
HZY006	*ulp2-SIM^{3A}, F839D, CCR^{3A}::kanMX6, derived from HZY621*	Albuquerque, et al, *JBC* 2018
PLASMID	DESCRIPTION	SOURCE
HZE2340	pRS315-Ulp2-TAF:: *kanMX6*	Albuquerque, et al, *JBC* 2018
HZE2341	pRS315-*ulp2-SIM^{3A}*-TAF:: *kanMX6*	Albuquerque, et al, *JBC* 2018
HZE2342	pRS315-*ulp2-F839D*-TAF:: *kanMX6*	Albuquerque, et al, *JBC* 2018
HZE2527	pRS315-*ulp2-CCR^{3A}*-TAF:: *kanMX6*	Albuquerque, et al, *JBC* 2018
HZE2343	pRS315-*ulp2-(SIM^{3A}, F839D)*-TAF:: *kanMX6*	Albuquerque, et al, *JBC* 2018
HZE2525	pRS315-*ulp2-(SIM^{3A}, CCR^{3A})*-TAF:: *kanMX6*	Albuquerque, et al, *JBC* 2018
HZE2526	pRS315-*ulp2-(F839D, CCR^{3A})*-TAF:: *kanMX6*	Albuquerque, et al, *JBC* 2018
HZE2439	pRS315-*ulp2-(SIM^{3A}, F839D, CCR^{3A})*-TAF:: *kanMX6*	Albuquerque, et al, *JBC* 2018
HZE1145	LIC-2BT-Ulp2-(400-767)	Albuquerque, et al, *JBC* 2018

HZE1142	LIC-2BT-*ulp2-SIM* ^{3A}-(400-767)	Albuquerque, et al, *JBC* 2018
HZE2346	Lic-2BT-Smt3 (1xSUMO)	Albuquerque, et al, *JBC* 2018
HZE2347	LIC-2BT-2xSmt3 (2xSUMO)	Albuquerque, et al, *JBC* 2018
HZE2348	LIC-2BT-4xSmt3 (4xSUMO)	Albuquerque, et al, *JBC* 2018
HZE2349	LIC-2BT-6xSmt3 (6xSUMO)	Albuquerque, et al, *JBC* 2018
HZE2585	pRS315-*ulp2 (PIASX-SIM, F839D, CCR*^{3A}*)*-TAF:: *kanMX6,* Ulp2-SIM (sequence IQII) is substituted by PIASX-SIM (sequence: VDVIDL)	Albuquerque, et al, *JBC* 2018
HZE2586	pRS315-*ulp2 (M-IR2-SIM, F839D, CCR*^{3A}*)*-TAF:: *kanMX6.* Ulp2-SIM (sequence IQII) is substituted by RanGAP M-IR2-SIM (sequence: VIIVW)	Albuquerque, et al, *JBC* 2018

References

Aillet, F., Lopitz-Otsoa, F., Egana, I., Hjerpe, R., Fraser, P., Hay, R. T., Rodriguez, M. S., Lang, V. (2012). Heterologous SUMO-2/3-ubiquitin chains optimize IkappaBalpha degradation and NF-kappaB activity. PLoS One, 7(12), e51672. doi:10.1371/journal.pone.0051672

Albuquerque, C. P., Wang, G., Lee, N. S., Kolodner, R. D., Putnam, C. D., & Zhou, H. (2013). Distinct SUMO ligases cooperate with Esc2 and Slx5 to suppress duplication-mediated genome rearrangements. PLoS Genet, 9(8), e1003670. doi:10.1371/journal.pgen.1003670

Albuquerque, C. P., Yeung, E., Ma, S., Fu, T., Corbett, K. D., & Zhou, H. (2015). A Chemical and Enzymatic Approach to Study Site-Specific Sumoylation. PLoS One, 10(12), e0143810. doi:10.1371/journal.pone.0143810

Andersen, J. S., Matic, I., & Vertegaal, A. C. (2009). Identification of SUMO target proteins by quantitative proteomics. Methods Mol Biol, 497, 19-31. doi:10.1007/978-1-59745-566-4_2

Bayer, P., Arndt, A., Metzger, S., Mahajan, R., Melchior, F., Jaenicke, R., & Becker, J. (1998). Structure determination of the small ubiquitin-related modifier SUMO-1. J Mol Biol, 280(2), 275-286. doi:10.1006/jmbi.1998.1839

Bylebyl, G. R., Belichenko, I., & Johnson, E. S. (2003). The SUMO isopeptidase Ulp2 prevents accumulation of SUMO chains in yeast. J Biol Chem, 278(45), 44113-44120. doi:10.1074/jbc.M308357200

Cremona, C. A., Sarangi, P., Yang, Y., Hang, L. E., Rahman, S., & Zhao, X. (2012). Extensive DNA damage-induced sumoylation contributes to replication and repair and acts in addition to the mec1 checkpoint. Mol Cell, 45(3), 422-432. doi:10.1016/j.molcel.2011.11.028

de Albuquerque, C. P., Liang, J., Gaut, N. J., & Zhou, H. (2016). Molecular Circuitry of the SUMO (Small Ubiquitin-like Modifier) Pathway in Controlling Sumoylation Homeostasis and Suppressing Genome Rearrangements. J Biol Chem, 291(16), 8825-8835. doi:10.1074/jbc.M116.716399

de Albuquerque, C. P., Suhandynata, R. T., Carlson, C. R., Yuan, W. T., & Zhou, H. (2018). Binding to small ubiquitin-like modifier and the nucleolar protein Csm1 regulates substrate specificity of the Ulp2 protease. J Biol Chem, 293(31), 12105-12119. doi:10.1074/jbc.RA118.003022

Elmore, Z. C., Donaher, M., Matson, B. C., Murphy, H., Westerbeck, J. W., & Kerscher, O. (2011). Sumo-dependent substrate targeting of the SUMO protease Ulp1. BMC Biol, 9, 74. doi:10.1186/1741-7007-9-74

Gillies, J., Hickey, C. M., Su, D., Wu, Z., Peng, J., & Hochstrasser, M. (2016). SUMO Pathway Modulation of Regulatory Protein Binding at the Ribosomal DNA Locus in Saccharomyces cerevisiae. Genetics, 202(4), 1377-1394. doi:10.1534/genetics.116.187252

Hannich, J. T., Lewis, A., Kroetz, M. B., Li, S. J., Heide, H., Emili, A., & Hochstrasser, M. (2005). Defining the SUMO-modified proteome by multiple approaches in Saccharomyces cerevisiae. J Biol Chem, 280(6), 4102-4110. doi:10.1074/jbc.M413209200

Hardeland, U., Steinacher, R., Jiricny, J., & Schar, P. (2002). Modification of the human thymine-DNA glycosylase by ubiquitin-like proteins facilitates enzymatic turnover. Embo j, 21(6), 1456-1464. doi:10.1093/emboj/21.6.1456

Hickey, C. M., Wilson, N. R., & Hochstrasser, M. (2012). Function and regulation of SUMO proteases. Nat Rev Mol Cell Biol, 13(12), 755-766. doi:10.1038/nrm3478

Hochstrasser, M. (2001). SP-RING for SUMO: new functions bloom for a ubiquitin-like protein. Cell, 107(1), 5-8.

Huang, J., & Moazed, D. (2003). Association of the RENT complex with nontranscribed and coding regions of rDNA and a regional requirement for the replication fork block protein Fob1 in rDNA silencing. Genes Dev, 17(17), 2162-2176. doi:10.1101/gad.1108403

Johnson, E. S., & Blobel, G. (1999). Cell cycle-regulated attachment of the ubiquitin-related protein SUMO to the yeast septins. J Cell Biol, 147(5), 981-994.

Johnson, E. S., & Gupta, A. A. (2001). An E3-like factor that promotes SUMO conjugation to the yeast septins. Cell, 106(6), 735-744.

Kroetz, M. B., Su, D., & Hochstrasser, M. (2009). Essential role of nuclear localization for yeast Ulp2 SUMO protease function. Mol Biol Cell, 20(8), 2196-2206. doi:10.1091/mbc.E08-10-1090

Li, S. J., & Hochstrasser, M. (1999). A new protease required for cell-cycle progression in yeast. Nature, 398(6724), 246-251. doi:10.1038/18457

Li, S. J., & Hochstrasser, M. (2000). The yeast ULP2 (SMT4) gene encodes a novel protease specific for the ubiquitin-like Smt3 protein. Mol Cell Biol, 20(7), 2367-2377.

Li, S. J., & Hochstrasser, M. (2003). The Ulp1 SUMO isopeptidase: distinct domains required for viability, nuclear envelope localization, and substrate specificity. J Cell Biol, 160(7), 1069-1081. doi:10.1083/jcb.200212052

Liang, J., Singh, N., Carlson, C. R., Albuquerque, C. P., Corbett, K. D., & Zhou, H. (2017). Recruitment of a SUMO isopeptidase to rDNA stabilizes silencing complexes by opposing SUMO targeted ubiquitin ligase activity. Genes Dev, 31(8), 802-815. doi:10.1101/gad.296145.117

Lima, C. D., & Reverter, D. (2008). Structure of the human SENP7 catalytic domain and poly-SUMO deconjugation activities for SENP6 and SENP7. J Biol Chem, 283(46), 32045-32055. doi:10.1074/jbc.M805655200

Matunis, M. J., Coutavas, E., & Blobel, G. (1996). A novel ubiquitin-like modification modulates the partitioning of the Ran-GTPase-activating protein RanGAP1 between the cytosol and the nuclear pore complex. J Cell Biol, 135(6 Pt 1), 1457-1470.

Mossessova, E., & Lima, C. D. (2000). Ulp1-SUMO crystal structure and genetic analysis reveal conserved interactions and a regulatory element essential for cell growth in yeast. Mol Cell, 5(5), 865-876.

Mukhopadhyay, D., Ayaydin, F., Kolli, N., Tan, S. H., Anan, T., Kametaka, A., Azuma, Y., Wilkinson, K. D., Dasso, M. (2006). SUSP1 antagonizes formation of highly SUMO2/3-conjugated species. J Cell Biol, 174(7), 939-949. doi:10.1083/jcb.200510103

Munk, S., Sigurethsson, J. O., Xiao, Z., Batth, T. S., Franciosa, G., von Stechow, L., Lopez-Contreras, A. J., Vertegaal, A. C. O., Olsen, J. V. (2017). Proteomics Reveals Global Regulation of Protein SUMOylation by ATM and ATR Kinases during Replication Stress. Cell Rep, 21(2), 546-558. doi:10.1016/j.celrep.2017.09.059

Nathan, D., Ingvarsdottir, K., Sterner, D. E., Bylebyl, G. R., Dokmanovic, M., Dorsey, J. A., Whelan, K. A., Krsmanovic, M., Lane, W. S., Meluh, P. B., Johnson, E. S., Berger, S. L. (2006). Histone sumoylation is a negative regulator in Saccharomyces cerevisiae and shows dynamic interplay with positive-acting histone modifications. Genes Dev, 20(8), 966-976. doi:10.1101/gad.1404206

Panse, V. G., Kuster, B., Gerstberger, T., & Hurt, E. (2003). Unconventional tethering of Ulp1 to the transport channel of the nuclear pore complex by karyopherins. Nat Cell Biol, 5(1), 21-27. doi:10.1038/ncb893

Reindle, A., Belichenko, I., Bylebyl, G. R., Chen, X. L., Gandhi, N., & Johnson, E. S. (2006). Multiple domains in Siz SUMO ligases contribute to substrate selectivity. J Cell Sci, 119(Pt 22), 4749-4757. doi:10.1242/jcs.03243

Reverter, D., & Lima, C. D. (2004). A basis for SUMO protease specificity provided by analysis of human Senp2 and a Senp2-SUMO complex. Structure, 12(8), 1519-1531. doi:10.1016/j.str.2004.05.023

Reverter, D., & Lima, C. D. (2005). Insights into E3 ligase activity revealed by a SUMO-RanGAP1-Ubc9-Nup358 complex. Nature, 435(7042), 687-692. doi:10.1038/nature03588

Reverter, D., & Lima, C. D. (2006). Structural basis for SENP2 protease interactions with SUMO precursors and conjugated substrates. Nat Struct Mol Biol, 13(12), 1060-1068. doi:10.1038/nsmb1168

Ryu, H. Y., Wilson, N. R., Mehta, S., Hwang, S. S., & Hochstrasser, M. (2016). Loss of the SUMO protease Ulp2 triggers a specific multichromosome aneuploidy. Genes Dev, 30(16), 1881-1894. doi:10.1101/gad.282194.116

Shen, L. N., Dong, C., Liu, H., Naismith, J. H., & Hay, R. T. (2006). The structure of SENP1-SUMO-2 complex suggests a structural basis for discrimination between SUMO paralogues during processing. Biochem J, 397(2), 279-288. doi:10.1042/bj20052030

Shiio, Y., & Eisenman, R. N. (2003). Histone sumoylation is associated with transcriptional repression. Proc Natl Acad Sci U S A, 100(23), 13225-13230. doi:10.1073/pnas.1735528100

Song, J., Durrin, L. K., Wilkinson, T. A., Krontiris, T. G., & Chen, Y. (2004). Identification of a SUMO-binding motif that recognizes SUMO-modified proteins. Proc Natl Acad Sci U S A, 101(40), 14373-14378. doi:10.1073/pnas.0403498101

Srikumar, T., Lewicki, M. C., & Raught, B. (2013). A global S. cerevisiae small ubiquitin-related modifier (SUMO) system interactome. Mol Syst Biol, 9, 668. doi:10.1038/msb.2013.23

Sriramachandran, A. M., & Dohmen, R. J. (2014). SUMO-targeted ubiquitin ligases. Biochim Biophys Acta, 1843(1), 75-85. doi:10.1016/j.bbamcr.2013.08.022

Takahashi, Y., Kahyo, T., Toh, E. A., Yasuda, H., & Kikuchi, Y. (2001). Yeast Ull1/Siz1 is a novel SUMO1/Smt3 ligase for septin components and functions as an adaptor between conjugating enzyme and substrates. J Biol Chem, 276(52), 48973-48977. doi:10.1074/jbc.M109295200

Wykoff, D. D., & O'Shea, E. K. (2005). Identification of sumoylated proteins by systematic immunoprecipitation of the budding yeast proteome. Mol Cell Proteomics, 4(1), 73-83. doi:10.1074/mcp.M400166-MCP200

Yunus, A. A., & Lima, C. D. (2009). Structure of the Siz/PIAS SUMO E3 ligase Siz1 and determinants required for SUMO modification of PCNA. Mol Cell, 35(5), 669-682. doi:10.1016/j.molcel.2009.07.013

Zhao, X., & Blobel, G. (2005). A SUMO ligase is part of a nuclear multiprotein complex that affects DNA repair and chromosomal organization. Proc Natl Acad Sci U S A, 102(13), 4777-4782. doi:10.1073/pnas.0500537102

Zhao, X., Wu, C. Y., & Blobel, G. (2004). Mlp-dependent anchorage and stabilization of a desumoylating enzyme is required to prevent clonal lethality. J Cell Biol, 167(4), 605-611. doi:10.1083/jcb.200405168